Direct Computation of Multi Valued Phase-Space Solutions for Hamilton-Jacobi Equations

Jean-David Benamou

INRIA

INSTITUT NATIONAL DE RECHERCHE EN INFORMATIQUE ET EN AUTOMATIQUE

Direct Computation of Multi Valued Phase-Space Solutions for Hamilton-Jacobi Equations

Jean-David Benamou

N ° 3414

Avril 1998

THÈME 4

ISSN 0249-6399

Direct Computation of Multi Valued Phase-Space Solutions for Hamilton-Jacobi Equations

Jean-David Benamou *

Thème 4 — Simulation et optimisation
de systèmes complexes
Projet Ondes

Rapport de recherche n°3414 — Avril 1998 — 45 pages

Abstract: A method is presented for the exact and complete resolution of Hamiltonian systems only using the corresponding Hamilton-Jacobi equation (we show that it possible to get the ODE solution from the corresponding PDE).

(Résumé : tsvp)

* INRIA, Domaine de Voluceau, B.P.105 78153 Le Chesnay cedex, France, e-mail :Jean-David.Benamou@inria.fr

Unité de recherche INRIA Rocquencourt
Domaine de Voluceau, Rocquencourt, BP 105, 78153 LE CHESNAY Cedex (France)
Téléphone : 01 39 63 55 11 - International : +33 1 39 63 55 11
Télécopie : (33) 01 39 63 53 30 - International : +33 1 39 63 53 30

Calcul direct de solutions multi valuées de l'espace des phases pour des équations d'Hamilton-Jacobi

Résumé : Nous présentons une méthode pour la résolution exacte et complète de systèmes Hamiltoniens qui utilise uniquement l'équation dHámilton-Jacobi correspondante

Contents

List of Figures

1 Introduction

We are interested in the *direct* computation of *multi valued phase-space* solutions of time dependent 1-D Hamilton-Jacobi equation ($g_{,x_1}(x_1,x_2)$ denotes the partial differentiation of g with respect to x_1) :

$$\begin{cases} \phi_{,t}(t,x) + H(t,x,\phi_{,x}(t,x)) = 0, \ in\ \Omega = \{(t,x) \in \mathbb{R}\times\mathbb{R},\ t > \gamma(x)\} \\ \phi(\gamma(x),x) = \phi^0(x),\ for\ x \in \mathbb{R}. \end{cases} \tag{1}$$

Cauchy data, in the form of a continuous function ϕ^0, is prescribed on the curve $\Gamma = \{(x,\gamma(x)),\ x \in \mathbb{R}\}$ which is Lipschitz regular. The restriction to a subset of $\mathbb{R}$ is discussed in section 4.5. The function $H(t,y,p)$ is called Hamiltonian. It is assumed to be continuous up to its second partial derivatives and strictly convex and coercive in its last variable p. The *phase-space* solution of this equation is defined using the corresponding Hamiltonian system :

$$\begin{cases} \dot{y}(s,x^0) = H_{,p}(s,y(s,x^0),p(s,x^0)) \\ \dot{p}(s,x^0) = -H_{,y}(s,y(s,x^0),p(s,x^0)) \\ \dot{\varphi}(s,x^0) = p(s,x^0).H_{,p}(s,y(s,x^0),p(s,x^0)) - H(s,y(s,x^0),p(s,x^0)) \\ y(\gamma(x^0),x^0) = x^0,\ p(\gamma(x^0),x^0) = p^0(x^0),\ \varphi(0,x^0) = \phi^0(x^0),\ for\ x^0 \in \mathbb{R}. \end{cases} \tag{2}$$

The dot stands for time derivation $\dot{(.)} = \frac{d(.)}{ds}$. We come back on the determination of p^0 and give additional conditions on ϕ^0, γ and H in section 2.1 (in the simple $\gamma \equiv 0$ case, $p^0(x) = \phi^0_{,x}(x^0)$). This system of ODEs generates, for all $x^0 \in \mathbb{R}$, bicharacteristic strips $(y(s,x^0),p(s,x^0))$ lying in phase-space $\mathbb{R}_y \times \mathbb{R}_p$ and depending continuously on t and x^0. The projections of the strips onto $\mathbb{R}_y$: $y(s,x^0)$ are called bicharacteristic curves.

An important quantity is the oriented measure of an infinitesimal area (in time and space) transported by bicharateristics :

$$D(y(s,x^0)) = ds \wedge dy(s,x^0) = \frac{\partial y(s,x^0)}{\partial x^0}(ds \wedge dx^0). \tag{3}$$

As long as :

$$D(y(s,x^0) \neq 0 \tag{4}$$

is non zero along a curve $y(s,x^0)$, the bicharacteristic field remains locally regular. It is possible to construct a smooth function $\tilde{\phi}(t,x)$ in a neighborhood of this curve such that :

$$\begin{cases} \tilde{\phi}_{,t}(t,x) + H(t,x,\tilde{\phi}_{,x}(t,x)) = 0, \\ \tilde{\phi}_{,x}(s,y(s,x^0)) = p(s,x^0),\ and \\ \tilde{\phi}(s,y(s,x^0)) = \varphi(s,x^0),\ for\ s > \gamma(x^0),\ in\ particular : \\ \tilde{\phi}(\gamma(x^0),x^0) = \phi_0(x^0), \end{cases} \tag{5}$$

This result justifies labeling solutions of (2) as phase-space solutions of (1). Note that, in the case of single valued phase space solutions (1) is equivalent to (5) and $\phi = \tilde{\phi}$.

Under reasonable hypothesis, it is always possible to solve directly the PDE (1). A generalized theory of *viscosity single valued* solution exists for such equations (see [CL83] or [Bar94] for a comprehensive review of such methods). It is complemented by a large number of numerical studies proposing stable finite differences or finite elements schemes commonly referred to as *upwind schemes* ([OS89] [RT88] [Set96] [SVST94] [Abg96]). This terminology express the idea that, like for hyperbolic conservation laws, the essential ingredient of these methods is to take into account the *upwind* information carried by the bicharacteristics (even though they are not computed). If bicharacteristic curves do not cross in position space $\mathbb{R}_y$, we obtain a *single valued* ϕ field. In this case, the viscosity solution of (1) matches the classical solution. When the phase-space solution of (2) is multi valued (i.e. bicharacteristics cross), the classical solution breaks down and the single valued viscosity solution develops singularities. The question of whether or not it is possible to compute the multi valued phase-space solutions using direct resolution of the PDE arise naturally. In other words, we want the solution of (2) without using the ODE *phase-space* technique.

This problem has been an active research subject in geometrical optics with potential applications in high frequency wave modeling for geophysics. The advantage of the PDE approach is to provide directly the solution ϕ on a regular grid spanning the domain of interest. A feature not shared by the ODE approach for which there is no a priori control on the shape of the bicharacteristics. Low density zones, reached by few bicharacteristics, are particularly problematic. However, the PDE approach only provide a *single valued* solution. Conversely the ODE approach computes the *multi valued phase-space* solution along the bicharacteristics. It is worth mentioning that the process of recovering the multi valued solution on a regular grid from the *phase-space* ODE solution relies on sophisticated interpolation and sorting techniques ([LLH96] [KKC94] [VIG93]). Hence the interest in designing a PDE-based method able to compute the multi valued solution for same or lower cost than existing ODE-based method. Such a method can find direct application in imaging technique such a migration or inversion ([GB93] [SS94] [BG85] [Bey85]). The link between first arrival travel-time and upwind viscosity solution of the Eikonal (Hamilton-Jacobi equation) solution was noticed in ([Vid88]) and assessed in ([TS91]). Then, several PDE-based algorithm were proposed to recover the *multi valued* solution : Some ideas presented in this paper are connected to [EFO95], we mention the link in section 7.2, 7.3; the identification of the different branches of the multi valued solution as "local" viscosity solution was studied in [Ben96] ; [Sym96] proposes to sort adjacent local viscosity solution with selected sources, also in order to recover multi valued solutions. A partial analysis of these algorithms can be found in [Ben97]. A different approach based on a kinetic formulation of the problem and called the moment method has been pursued in [BL96] [ER95]. Finally let us mention related works trying to cope with the difficulties associated with multi valued travel-time

fields : [EFO] [per].

The idea of this paper is that the multi valued phase-space solution can be split into solutions of (1) using condition (4). We are considering each of the different branches of the multi valued solution as PDE-solutions with ad-hoc boundary and initial conditions. The method relies on the generic classification of singularities of Lagrangian/Legendrian submanifolds associated to first order Hamilton-Jacobi equations ([AGZV86] [Izu93]). We show that, based on this generic qualitative information, it is possible to *automatically* detect singularities giving rise to *multi valued* solutions and *adaptatively* generate all branches of the solution.

Organization of the paper :
Section 2 : The problem is reformulated in the framework of calculus of variation. The bicharacteristics can then be interpreted as extremals of a least action principle. The distinction between minima and other type of extremals rely on the notion of conjugate points. The value function taken by the action along the bicharacteristics solves the *multi valued* Hamilton-Jacobi equation.
Section 3 : We review the differential geometry approach to the problem. In this framework bicharacteristics span a Lagrangian/Legendrian submanifold in phase-space. The singularities of the projection of this manifold onto position space $\mathbb{R}_y$, called caustics, give rise to *multi valued* solutions of (1). A generic classification of these singularity is available.
Section 4 : We review the PDE-approach based on viscosity solutions. Viscosity solutions can be characterized using deterministic optimal control theory. We also show it is possible to derive a PDE which, when coupled to (1) can be used to locate caustic/conjugate points.
Section 5 : We provide a theoretical justification of the splitting of the multi valued solution into viscosity solutions of (1). This is based on the generic classification of section 3 and on the characterization both of the multi valued solution in section 2 and the viscosity solution in section 4.
Section 6 : describes the core of our algorithm and its numerical implementation. We explain how it can be used recursively to treat the general case.
Section 7 : We discuss potential generalizations and open problems.
Section 8 : We apply our method to geometrical optics and provide numerical results. Section 9 : Conclusion.

Section 2 to 4 are to be considered as preliminaries needed to understand our main result in section 5 and the numerical algorithm in section 6. These preliminary results are sometime shared and often scattered between different schools and communities. We tried, in order to make this paper self content, to give a minimal overview of the material needed. These sections are not to be considered as a detailed review or a rigorous exposition of the results of these different theories.

2 The Calculus of variation approach

We review here classical results of calculus of variation which can be found, for instance, in [GF63] [You69].

2.1 Finding the extremals

Let us first introduce the Legendre transform $H^\star$ of H as :

$$L(t,x,v) = H^\star(t,x,v) = \sup_{p\in\mathbb{R}_p} \{p.v - H(t,x,p)\}$$

The coercivity and convexity assumptions ensure that L is well defined, proper and satisfies :

$$H(t,x,p) = \sup_{v\in\mathbb{R}_p} \{p.v - H^\star(t,x,p)\}. \tag{6}$$

A classical duality result states that $L_{,v}$ and $H_{,p}$ are inverse functions. Then, the strict convexity of H implies :

$$L_{,vv} > 0 \tag{7}$$

is a positive definite matrix (simply a scalar in 1-D). Equation (6) is the classical Lagrangian/Hamiltonian duality needed to obtain the following result : finding the multi valued solution of (2) is equivalent to finding, for all $(t,x) \in \Omega$, the extremals of the minimization problem

$$\inf_{\{\alpha\in\mathbb{R},\, y(.)\in C^1(\mathbb{R});\, y(\gamma(\alpha))=\alpha,\, y(t)=x\}} J^{(t,x)}(\alpha,y) = \int_{\gamma(\alpha)}^{t} L(s,y(s),\dot{y}(s))ds + \phi^0(\alpha). \tag{8}$$

The admissible curves $y(.)$ are smooth (C^1 in the framework of "weak extrema") and constrained to connect a point of Γ: $(\gamma(\alpha),\alpha)$ for some $\alpha \in \mathbb{R}$, to (t,x) in Ω. The extremals of this problem are characterized, for all α, by the system :

$$\begin{cases} L_{,x}(s,y(s),\dot{y}(s)) - \frac{d}{ds}L_{,v}(t,y(s),\dot{y}(s)) = 0, \\ y(\gamma(\alpha)) = \alpha, \\ L_{,v}(\gamma(\alpha),\alpha,\dot{y}(\gamma(\alpha))) + ... \\ \gamma_{,x}(\alpha)(L(\gamma(\alpha),\alpha,\dot{y}(\gamma(\alpha))) - \dot{y}(\gamma(x))L_{,v}(\gamma(\alpha),\alpha,\dot{y}(\gamma(\alpha))) = \phi^0_{,x}(\alpha), \\ y(t) = x. \end{cases} \tag{9}$$

These equations express the cancellation of the first variation of J with respect to α and y. We use the compact notation $J_{,\alpha} = 0$ and $J_{,y} = 0$. The first line of (9), called the Euler/Lagrange equation, corresponds *exactly* to the first two ODE in system (2). The following lines, called the transversality conditions, determine the initial conditions on y and p.

We can identify the solutions of (2) with the extremals of problem (8) set for $(t,x) = (t, y(t,x^0))$. More precisely :

Proposition 2.1 *We have, for all t and all x^0 :*

$$\begin{cases} J_{,\alpha}^{(t,y(t,x^0))}(x^0, y(.,x^0)) = 0, \\ J_{,y}^{(t,\alpha(t,x^0))}(x^0, y(.,x^0)) = 0. \end{cases}$$

Proof : Setting $p(s) = L_{,v}(t, y(s), \dot{y}(s))$, and using (7) it is a classical exercise in the calculus of variation to recover the ODEs of system (2) from the first equation of the proposition. It is now enough to show that the initial conditions of (2) and (9) match. It is obvious for the initial condition on y. Concerning p we must check the third equation of (9) to be equivalent to to setting of p^0 in (2). More precisely we want :

$$p^0(\alpha) = L_{,v}(\gamma(\alpha), \alpha, \dot{y}(\gamma(\alpha))). \tag{10}$$

We first have to specify how we chose the initial condition on p^0 in (2) such that our phase-space solution corresponds to the Cauchy data ϕ^0 of (1). It is known that classical solution to (1) can always be defined for arbitrary small time. It means that, in a neighborhood of Γ, we can write $\phi_{,x}(s, y(s,\alpha)) = p(s,\alpha)$ (see (5)). Differentiating the initial condition and using the equation in (1) we get that p^0 must satisfy :

$$-\gamma_{,x}(\alpha)H(\gamma(\alpha), \alpha, p^0(\alpha)) + p^0(\alpha) = \phi^0_{,x}(\alpha). \tag{11}$$

If $\gamma_{,x}(\alpha) = 0$, we unambiguously have $p^0(\alpha) = \phi^0_{,x}(\alpha)$. Under the additional assumptions :

$$\begin{cases} -\gamma_{,x}(\alpha)H(\gamma(\alpha), \alpha, p) + p \to +\infty \; as \; p \to +\infty, \; if \; \gamma_{,x} \geq 0, \\ -\gamma_{,x}(\alpha)H(\gamma(\alpha), \alpha, p) + p \to -\infty \; as \; p \to -\infty, \; if \; \gamma_{,x} \leq 0, \end{cases} \tag{12}$$

equation (11) has a unique solution $p^0(\alpha)$ satisfying $-\gamma_{,x}(\alpha)H_{,p}(\gamma(\alpha), \alpha, p^0(\alpha)) \geq 0$. It guarantees that the bicharacteristics point into Ω (we recall that $\dot{y} = H_{,p}$). Replacing p^0 in (11) using (10), we exactly recover the transversality condition on p in (9). This proves (10).

Remark 2.2 *We want to emphasize that the bicharacteristics can therefore be globally called extremals of our variational problem (8). We mean that curves are extremals for any end point $(t, y(t, x^0))$ $t > \gamma(x^0)$. See also remark 2.5.*

Remark 2.3 *A sufficient conditions on H to satisfy (23) is , for example, $H(t,x,p) \sim C|p|$ when $p \to \pm\infty$ (H is coercive) and $|\gamma_{,x}| < \frac{1}{C}$. We can relax these assumptions with additional hypothesis on ϕ^0.*

2.2 Conjugate points and sufficient conditions for a minimum

Condition (7) :

$$L_{,vv}(s, y(s), \dot{y}(s)) > 0 \tag{13}$$

holds for any extremal curve $y(.,x^0)$, between $y(\gamma(x^0),x^0)$ and $y(t,x^0)$ for all t. A necessary and sufficient condition for this curve to be a minimum for the minimization of $J^{(t,y(t))}(\alpha,y)$:

$$J^{(t,y(t,x^0))}(x^0,y(.,x^0)) = \inf_{\{\alpha\in\mathbb{R},\ y(.)\in C^1(\mathbb{R});\ y(\gamma(\alpha))=\alpha,\ y(t)=x\}} J^{(t,x)}(\alpha,y),$$

is the *absence of conjugate points* on this portion of curve. The presence of a conjugate point on the curve exactly means that the second variation of $J^{(t,y(t,x^0))}$ with respect to y is a non positive definite quadratic functional. An important remark is :

Conjugate points can be shown to be points where the non degeneracy condition (4) fails. Such points also corresponds to caustic points (next section).

Remark 2.4 *There is an intimate connection between conjugate/caustic points, the occurrence of multi valued solutions and consequently the failure of the classical Hamilton-Jacobi interpretation (1).*

Remark 2.5 *Let us consider the case of only one conjugate point $y^c = y(t^c,x)$ on an extremal curve $y(.,x)$ starting at $s=\gamma(x^0)$. The above results asserts that for $t > t^c$ this curve is not a minimum. However, it is a minimum* before *the conjugate point (until $t \geq t^c$). Considering the same curve $y(.,x)$ but starting at $s = t^c$, we know there are no conjugate point on this section. Therefore, for the portion of curve lying after the conjugate point, the curve is a minimum.*

2.3 The value function and the Hamilton-Jacobi equation

Another important feature of problem (8) is the interpretation of the value function as the phase-space solution of the Hamilton-Jacobi equation (1) along the extremals :

$$J^{(t,y(t,x^0))}(x^0,y(.,x^0)) = \varphi(t,x^0) \tag{14}$$

As pointed out in the introduction, this interpretation fails as soon as multi valuedness occurs. Basically this means that bicharacteristic curves cross in position space $\mathbb{R}_y$. One must carefully distinguish between two situations. The failure of the local condition (4) at a caustic point precisely means that the projection of neighboring bicharacteristic *strips* onto position space cross. Crossing between such projections of bicharacteristic *curves* may also happen for curves that are not close in phase-space. In this case the bicharacteristics cross in position space (y) with different momentum (p). It generates singularities called kinks (or shocks by analogy with hyperbolic conservation laws) in the viscosity solution (see also section 5.2).

3 The differential geometry approach

Simplectic differential geometry is a useful tool to classify multi valued solutions of first order Hamilton Jacobi equations. We do not get into the details and follow closely [IK] and [KSV] to provide material needed in the sequel of the paper. Fore more on this topic one can see [AGZV86] [Izu93] [Dui74]. An intuitive presentation of simplectic geometry can also be found in [Arn92].

3.1 The Lagrangian/Legendrian submanifold and its projection

The Hamilton-Jacobi equation is defined as an hypersurface :

$$E(H) = \{(t, y, \phi, q, p) \in J^1(\mathbb{R} \times \mathbb{R}^n, \mathbb{R});\ q + H(t, y, p) = 0\}$$

where $J^1(\mathbb{R} \times \mathbb{R}^n, \mathbb{R})$, the space of 1-jet bundle of function of n variables, can be considered as $\mathbb{R}^5$ for $n = 1$ (our paper). Any "geometric" multi valued solution of $E(H)$: $\Lambda = \{(s, y(s, x^0), \phi(s, x^0), -H(s, y(s, x^0), p(s, x^0));\ \forall (s, x^0)\ s.\ t.\ s > \gamma(x^0)\}$, is a Legendrian submanifold in $J^1(\mathbb{R} \times \mathbb{R}^n, \mathbb{R})$ lying in $E(H)$. The similar framework of Lagrangian submanifold lie in phase-space and omits the phase function ϕ. In this case and for 1-D problems, $\Lambda = \{(s, y(s, x^0), -H(s, y(s, x^0), p(s, x^0));\ \forall (s, x^0)\ s.\ t.\ s > \gamma(x^0)\}$ is a 2-dimensional submanifold lying in the 4-dimensional phase-space (t, y, q, p).

Next we introduce the canonical projection mapping :

$$\begin{aligned} \Pi\ :\ \ & J^1(\mathbb{R} \times \mathbb{R}^n, \mathbb{R}) \longrightarrow \mathbb{R} \times \mathbb{R}^n \times \mathbb{R} \\ & (t, y, \phi, q, p) \longrightarrow (t, y, \phi). \end{aligned}$$

Finding the generic singularities/caustics of the solution consists in determining with respect to the time parameter t the location y of the generic bifurcations of the "wave fronts" : $t \rightarrow \Pi(E(H) \cap \Lambda)$. These so-called stable singularities (we refer to the above references for the "not so obvious" notion of stability) corresponds to the points where $D(y(s, x^0))$ (see 3) changes its sign and therefore fails to satisfy condition (4). The change of sign in $D(y(s, x^0)$ indicate that the infinitesimal area has shrinked to 0 and then changed its orientation. It happens at points where the Lagrangian submanifold "folds" in phase space and the its projection Π onto position space becomes singular.

3.2 Generic classification of caustics

It is possible to classify for the stable singularities of the projection Π. Modulo a diffeomorphism of the phase-space coordinates (t, y, q, p) into normal coordinates for which we use the same notation, we know the exact analytical canonical form of the Lagrangian manifold Λ in the neighborhood of such singularities/caustics. In the 1-D case (our paper) there is only one possibility, classified as the A_3 singularity and called *cusp*. The canonical form of the phase function is :

$$\phi(t, y, q, p) = \frac{1}{4}p^4 - \frac{1}{2}tp^2 + yp. \tag{15}$$

The restriction of the manifold Λ in phase- space (t, y, q, p) (Lagrangian submanifold) is locally described by :

$$\begin{cases} y = -p^3 + tp, \\ q = -\frac{1}{2}p^2. \end{cases} \tag{16}$$

Finally, condition (4) can be shown to be equivalent to $\frac{\partial \phi^2}{\partial q^2} = 0$ which, in our case reads :

$$t = +3p^2. \tag{17}$$

Remark 3.1 *Similar classifications exist in higher dimensions. In 2-D, one must consider two additional generic singularities called A_4 and $D_4^{\pm}$. These different types of singularities can be traced back to the different degeneracies of a Jacobian matrix which generalizes (3) (more in section 8.1). Information on the hierarchy in the apparition of singularities, called adjacency of singularity is available.*

3.3 Detailed structure of the cusp

We proceed to explain the analytical form of the singularity and the multi valued solution. Degeneracy condition (17) coupled to the manifold equations (16) gives the equation of the caustic curve in the (t, y) space :

$$t = \pm \frac{2}{3^{\frac{3}{2}}} y^{\frac{3}{2}}$$

This curve, pictured in figure 1, is called the cusp and is the only local generic singularity of Π in our case. It is formed of two convex curves Cr and Cl joining at a singular point (t_1, x_1) we call the cusp vertex. It is also possible to plot the multi valued phase function $\phi(t, y)$. The variable p is eliminated from (15) using the first equation of (16). This equation has exactly three real roots depending on (t, y) inside the cusp (i.e. for $-\frac{2}{3^{\frac{3}{2}}} y^{\frac{3}{2}} \leq t \leq \frac{2}{3^{\frac{3}{2}}} y^{\frac{3}{2}}$). On the caustic, two of these roots are identical and at the cusp vertex the three are the same. Figure 2 a) shows for successive times the plot of the phase ϕ as a function of y. One can observe the bifurcation at time t_1 leading to a triple-valued (triplication) phase function. Point S indicate a kink (or shock) in the associated viscosity solution and points C a caustic point. Caustic points separate the solution into *three single valued branches* (figure 5).

We are also interested in the bicharacteristic curves. Recall that they satisfy $\dot{y}(s, x^0) = H_{,p}(s, y(s, x^0), p(s, x^0))$ Using that bicharacteristics lie on $\Lambda \cap E(H)$ we get, using the second equation in (16) :

$$H_{,p}(t, y, p) = -q_{,p} = p.$$

Therefore, the three solutions for p of the first equation in (16) correspond locally to the vector field $\dot{y}$. We represent this multi valued vector field in figure 2 b) (the y scale is no the same as in a)). As expected, problems occur at the caustic points where $p_{,y}$ becomes infinite. Note, however, that the solution stays smooth in phase space (p, y). One can also precisely identify each branch of ϕ to the corresponding branch of p (more details on this in

section 5) and check that $\phi_x = p$ holds locally.

Using this information, we plot (figure 2 c)) 6 of these bicharacteristics in (t,y) space. Until time t_1 the solution is smooth and single valued, the bicharacteristics do not cross. At time t_1 a singularity appears at the cusp vertex. Characteristics cross there, $p_{,y}$ become infinite and the phase function has a singularity but there is no multi valuedness yet. After this time, the "triplication" develops. Each characteristics eventually touch tangentially the caustic (at points C) and then cross, at each point inside the cusp, two other bicharacteristics which have not yet touched the caustic (points T). At the S points two bicharacteristics cross with same associated phase *before* they have reached the caustic, *except at the cusp vertex. Reaching the caustic* for a bicharacteristic does not mean to cross the caustic but to touch it tangentially. This is where the Lagrangian submanifold folds in phase-space.

Finally let us mention two useful identities satisfied by this analytical solution. On the caustic, we have :

$$\begin{cases} (\phi_{,t}, \phi_{,y}).\nu = 0, \\ (\frac{\partial y(s,x^0)}{\partial x^0}, \frac{\partial p(s,x^0)}{\partial x^0}) = (0,0)^T. \end{cases} \tag{18}$$

where ν is the normal to the caustic curve in (t,y) space. The first equation means that contour lines of ϕ in (t,y) space are orthogonal to the caustic and the bicharacteristic curves tangent to the caustic (see figure 2 c). The second one that the projection (Π) of bicharacteristic *strips* cross at the caustic, i.e bicharacteristic curves cross with same momenta p and $D(y(s,x^0)$ changes of sign.

Remark 3.2 *The curves plotted in figures 1 to 6 give* qualitative *informations on the structure of the cusp and the geometric solution. They do not correspond to actual plots of the above analytical formulae.*

3.4 Cusps interactions

The multi valued geometric solution can, of course, be much more complicated. It occurs when several cusps are present. We show in figure 3 different possibilities with two cusps. The first situation a) is when the two cusps have no overlap. The solution simply develops triplication in each of these cusps. Case b) shows the possibility of an overlap between the cusps. The multi valued solution has five branches in the overlap. Finally case c) corresponds to the apparition of a new cusp in the last branch of the first one. Again there are 5 branches inside the new cusp. We further discuss these topics in section 6.5.

4 The PDE approach

The multi valued solution we want to compute has now been clearly identified through different approaches. We are about to investigate the nature and properties of the solutions

which can be recovered by simply solving the Hamilton-Jacobi equation considered as a PDE. While the theory goes back to [CL83], a review on this subject can be found in [Bar94] and also [FS93].

4.1 Viscosity solutions of Hamilton-Jacobi and the optimal control characterization

We are interested in the viscosity solution of problem (1) because the output of stable numerical schemes for such equation are known to converge to this class of solution (we refer to [RT88] [Bar94] [Abg96] for references on convergence studies). The viscosity solution moreover coincides with the classical smooth solution when there are no singularities. The results of this section have been adapted from [Bar94]. It relies on Bellman's equation for *exit time deterministic optimal control* problems. Let us consider, for (t,x) in Ω, the dynamical system :

$$\begin{cases} \dot{z}^{(t,x)}(s) = v(s), \ for \ s > t, \\ z^{(t,x)}(t) = x, \end{cases} \tag{19}$$

where $v(.)$ is a L^∞ function taking its value in $\mathbb{R}$. We define the exit time minimization problem :

$$\psi(t,x) = \inf_{v(.)} \{ \int_t^\tau L(s, z^{(t,x)}(s), v(s)) ds + \phi^0(z^{(t,x)}(\tau)) \} \tag{20}$$

where $\tau = \inf\{s > t; \ s = \gamma(z^{(t,x)}(s))\}$ is the first exit time of Ω trough Γ. Then, ψ is the *unique viscosity solution* of the Hamilton-Jacobi-Bellman equation :

$$\begin{cases} \psi_{,t}(t,x) + \sup_{v \in \mathbb{R}} \{ \psi_{,x}(t,x) v - L(t,x,v) \} = 0, \ in \ \Omega = \{(t,x) \in \mathbb{R}^+ \times \mathbb{R}, \ t > \gamma(x)\} \\ \psi(\gamma(x), x) = \phi^0(x), \ for \ x \in \mathbb{R}. \end{cases} \tag{21}$$

which is, of course, equivalent to (1) (use (6)).

Remark 4.1 *Theorem 5.3 in [Bar94] is originally formulated for a 2-D Dirichlet problem. It can easily be rewritten as a 1-D time dependent problem. The original theorem also includes an actualization cost depending on a parameter $\lambda > 0$. We can here relax this condition and take $\lambda = 0$ because we are in the unstationary case.*

4.2 The bicharacteristics interpretation

We make the link with the calculus of variation approach of section 1. Let us recall that extremals of problem (8), solutions of (2), are C^1 curves :

$$\begin{aligned} y(., x^0) \ : \ & \gamma(x^0) \longrightarrow t \\ & x^0 \longrightarrow y(t, x^0) = x. \end{aligned} \tag{22}$$

On the other hand, admissible curves for problem (20) have Lipschitz regularity and satisfy :

$$\begin{aligned} z^{(t^1,x)}(.) \ : \quad & t^1 \longrightarrow \tau = \gamma(z^{(t^1,x)}(\tau)) \ (exit\ time) \\ & x \longrightarrow z^{(t^1,x)}(\tau). \end{aligned} \tag{23}$$

Changing the time parameterization of (23) in order to match the structure of (22), it is possible to reformulate the optimal control problem (20) :

Proposition 4.2 *Problem (20) is equivalent to :*

$$\inf_{\{\alpha\in\mathbb{R},\ y(.)\in W^{1,+\infty}(\mathbb{R});\ y(\gamma(\alpha))=\alpha,\ y(t)=x\}} J^{(t,x)}(\alpha,y) = \int_{\gamma(\alpha)}^{t} L(s,y(s),\dot{y}(s))ds + \phi^0(\alpha). \tag{24}$$

Proof : We simply remark that any admissible curve (23) can be expressed as an admissible curve $y(.)$ for (24) through the change of variable

$$\begin{cases} \alpha = z^{(t^1,x)}(\tau), \\ t = 2\tau - t^1, \\ y(s) = z^{(t^1,x)}(s - \tau + t^1). \end{cases} \tag{25}$$

A reciprocal change of variable shows the converse to be also true. Under this change of variable, the cost functions for these two problems are identical.

The difference between (8) and (24) is the regularity of the admissible curves. In [GF63], curves (22) are called "weak extrema" because, the C^1 topology restricts the number of admissible curves compared to the C^0 topology for instance. Extrema for this last topology have been studied under the name of "strong" extrema. We extract from [GF63] the following result explaining the link between weak and strong minima :

Proposition 4.3 *Let $y(.,x^0)$ be an minimum for problem (8). It means in particular that (7) is satisfied and there are no conjugate/caustic points on this curve, (i.e. (4) is satisfied for $\gamma(x^0) < s < t$). Then,*

$y(.,x^0)$ is a strong *minimum for problem (8).*

The immediate corollary of this result is : Lipschitz ($W^{1,+\infty}$) curves being C^0, such a minimum is also a minimum for problem (20) (via proposition (4.2)). It also provides extra (C^1) regularity for the minima of problem (24). If only one curve solution of (2) reaches point (t,x) from $(\gamma(x^0),x^0)$ then the minimum is an absolute minimum and the viscosity solution ψ satisfies (thanks to (14)):

$$\psi(t,x) = \varphi(t,x^0) \tag{26}$$

If more than one minimal bicharacteristic reaches (t,x), we note $(\gamma(x_i^0),x_i^0)_{i=1..k}$ the k initial points of these curves. Then, the viscosity solution ψ selects the absolute minimum out of the relative minima :

$$\psi(t,x) = \min_{i=1..k} \varphi(t,x_i^0) \tag{27}$$

4.3 A 2-D Dirichlet/Neumann problem

A mentioned in remark 4.1, we can consider the 1-D time dependent Hamilton-Jacobi equation as a 2-D stationary equation. The results of section 4.1-4.2 can be extended to a more general problem (encountered in section 5) set the 2-D (t,x) space :

$$\begin{cases} \psi_{,t}(t,x) + \sup_{v\in\mathbb{R}}\{\psi_{,x}(t,x)v - L(t,x,v)\} = 0, \ in\ \Omega, \\ \psi(t,x) = \phi^0(x), \ on\ \Gamma^D, \\ (\phi_{,t},\phi_{,x}).\nu = 0, \ on\ \Gamma^N \end{cases} \tag{28}$$

where the boundary conditions on $\partial\Omega = \Gamma^D \cup \Gamma^N$ are mixt Dirichlet/Neumann boundary conditions and ν is the exterior normal. Like in section 4.1, ψ can be shown to solve the exit time optimal control problem (19) (20) with exit on Γ^D. The dynamical system is unchanged *except* when curves reach Γ^N where they are reflected symmetrically with respect ν (see theorem 5.10 in [Bar94]).

Using the arguments contained in section 4.2, it is possible to show that (26) and (27) hold *if* we consider the bicharacteristic curves $y(.,x^0)$ which are minima. Note that C^1 curves only satisfy the reflecting boundary condition when tangent to a convex boundary. It is exactly be the case for the bicharacteristics reaching the caustic (see (18) and figure 2 c).

Remark 4.4 *This problem corresponds to the free boundary problem of section 6.2. The free boundary is exactly the Neumann boundary of (28). We explain how we can numerically revert to a 1-D time dependent problem in section 6.4. See also remark 5.4.*

4.4 A transport equation for caustic detection

The locus of conjugate/caustic points is needed for our purpose of building the multi valued phase-space solution using the viscosity solution ψ. Even though section 3 provide a generic description of the caustic, this is a qualitative information. We derive here a numerically usable equation to compute $D(y(s,x^0))$ (see (3)).

The components actually needed to compute D are $(\frac{\partial y(s,x^0)}{\partial x^0}, \frac{\partial p(s,x^0)}{\partial x^0})$. We assume the domain, we are interested in, has constant D sign, this is the case until $D=0$. It automatically closes the domain at caustics. These quantities can, on one hand, be computed by

differentiating system (2) with respect to x^0 :

$$\left\{\begin{array}{l} \frac{\partial \dot{y}}{\partial x^0}(s,x^0) = H_{,py}(s,y(s,x^0),p(s,x^0))\frac{\partial y}{\partial x^0}(s,x^0) + ... \\ H_{,pp}(s,y(s,x^0),p(s,x^0))\frac{\partial p}{\partial x^0}(s,x^0), \\ \frac{\partial \dot{p}}{\partial x^0}(s,x^0) = -H_{,yy}(s,y(s,x^0),p(s,x^0))\frac{\partial y}{\partial x^0}(s,x^0) - ... \\ H_{,yp}(s,y(s,x^0),p(s,x^0))\frac{\partial p}{\partial x^0}(s,x^0) \\ \frac{\partial y}{\partial x^0}(\gamma(x^0),x^0) = 0,\ \frac{\partial p}{\partial x^0}(\gamma(x^0),x^0) = \frac{\partial p^0}{\partial x^0}(x^0). \end{array}\right. \tag{29}$$

On the other hand, instead of solving this set of ODE, we can derive a partial differential equation equivalent to (29) (like deriving (5) from (2)). Let us set introduce a nww variable, defined in time and space ($.^T$ is the transpose of .) :

$$\delta(t,y(t,x^0)) = (\frac{\partial y(t,x^0)}{\partial x^0}, \frac{\partial p(t,x^0)}{\partial x^0})^T,$$

and

$$A(t,y(s,x^0),p(s,x^0)) = \left(\begin{array}{cc} H_{,py}(s,y(s,x^0),p(s,x^0)) & H_{,pp}(s,y(s,x^0),p(s,x^0)) \\ -H_{,yy}(s,y(s,x^0),p(s,x^0)) & -H_{,yp}(s,y(s,x^0),p(s,x^0)) \end{array}\right)$$

Then, $\delta(t,x)$ can be uniquely defined everywhere (in the viscosity sense) and can be shown to satisfy the transport equation :

$$\left\{\begin{array}{l} \delta_{,t}(t,x) + H_{,p}(t,x,\phi_{,x})\delta_{,x}(t,x) = A(t,x,\phi_{,x}(x)).\delta(t,x), \\ \delta(\gamma(x),x) = (0, \frac{\partial p^0}{\partial x}(x)),\ for\ x \in \mathbb{R}. \end{array}\right. \tag{30}$$

This system, when coupled to (1) gives the necessary information to compute $D(t,x) = \delta(t,x)[1]$ (the first component of δ. In section 5, we use this coupling technique until we encounter a curve where $D = 0$. This strategy defines a free boundary problem.

Remark 4.5 *The key idea of his section is to replace the Lagrangian unknown $D(y(s,x^0))$ by the Eulerian quantity $D(t,x)$ depending on time and space. It is legitimate to do so using our method because it avoids dealing with multi valued and singular solutions (at caustics).*

4.5 Outgoing Boundary conditions

An interesting by-product (also for higher dimensions) of section 4.1 is the construction of outgoing boundary conditions to "close" our, yet unbounded, domain Ω. Let us "close" the domain Ω say on the "left" using a curve $\Gamma^\infty = \{(t,x^\infty);\ t \geq \gamma(x^\infty)\}$. We further assume that the bicharacteristic curves satisfy :

$$\dot{y}(s,x^0)) < 0,\ on\ \Gamma^\infty, \tag{31}$$

i.e, on Γ^∞, bicharacteristics can only *exit* the new domain $\Omega^\infty = \Omega \cap \{(t,x);\ x > x^\infty\}$. We now introduce the Dirichlet problem :

$$\begin{cases} \psi_{,t}(t,x) + \sup_{v\in\mathbb{R}}\{\psi_{,x}(t,x)v - L(t,x,v)\} = 0,\ in\ \Omega^\infty, \\ \psi(t,x) = \phi^0(x),\ for\ (t,x) \in \Gamma, \\ \psi(t,x) = +\infty,\ for\ (t,x) \in \Gamma^\infty. \end{cases} \tag{32}$$

For simplicity, we used Γ and Γ^∞ to denote respectively the parts of the boundary of Ω^∞ corresponding to the old Γ (Cauchy data/source) and to the new out-going boundary.

The optimal control characterization of section 4.2 (20) and condition (31) show that the viscosity solution of (32) matches the restriction of the viscosity solution of (1) to Ω^∞. Simply because the exit cost in (20), actually an entering cost for the bicharacteristics, takes an infinite value on Γ^∞. It therefore bars out any admissible curves starting on Γ^∞ and only takes into account curves issued from Γ as in the original unbounded problem.

Remark 4.6 *In practice $\phi = C$ on Γ^∞ (C big) is sufficient. Problem (32) can be seen as a Dirichlet problem with discontinuous boundary conditions. Even though this problem does not seems to satisfies the classical hypothesis for the existence and uniqueness of a viscosity solution, numerical experiments indicate the problem is well posed and indeed corresponds to the deterministic optimal control characterization (section 4.1). The condition $\phi = \infty$ also corresponds to Soner boundary condition [Son86].*

5 Splitting the multi valued solution

Our main objective is to show how a multi valued solution can be split and computed using viscosity solutions of (1). We use the information on the *structure* of the solution provided in section 3.3 and actually perform the analysis for *any* cusp caustic, which is locally diffeomorphically equivalent to the generic singularity A_3.

5.1 Smooth single valued solution

We focus first on the simplest case where the phase-space solution of (2) coincide with the classical smooth solution of (1). In this case (4) is satisfied in all Ω (D keeps constant sign). All bicharacteristic curves are actually absolute minima for problem (8) and (26) ensures that the viscosity solution of (1) is indeed the classical solution we are looking for. On figure 2 c), this is the case until time $t = t_1$ when the cusp vertex appears.

5.2 Singular single valued solution with shocks

If one just continues to solve for the viscosity solution after $t = t_1$. The solution forms a kink (or shock) curve where the bicharacteristics cross with same phase (before they reach

the caustic). The kink curve separate the cusp in two (figure 4). This can be inferred from (27) and section 3.3. See also [IK] on the generic classification of viscosity solution for Hamilton-Jacobi equation.

5.3 Multi valued solution

We turn to the solution with Cauchy initial data prescribed on $t = t_1$, precisely when the solution becomes multi valued. We note ϕ^1 the initial data. It can be computed as indicated in section 5.1.

Let $x = x_1$, the position of the cusp vertex (by analogy with t_1 its time coordinate), be known. Then the caustic can be separated at the cusp vertex in two parts. A right and and a left part noted $Cr = \{(\gamma^{Cr}(x), x);\ for\ x \geq x_1\}$ and $Cr = \{(\gamma^{Cl}(x), x);\ for\ x \leq x_1\}$ where γ^{Cr} and $= \gamma^{Cl}$ are the equation of the caustic (given). We classify the different smooth branches of the geometric multi valued solution as pictured on figure 5 :

- $-Cl$: is the portion of the solution corresponding to the bicharacteristics, issued at $t = t_1$ from the left of the cusp vertex ($x \leq x_1$), until they reach Cr.
- $-Cr$: is the portion of the solution corresponding to the bicharacteristics, issued at $t = t_1$ from the right of the cusp vertex ($x \geq x_1$), until they reach Cl.
- $+C$: is the solution associated to the remaining portion of the bicharacteristics (issued from Cl and Cr after the caustic).

Note that $-Cl$, $-Cr$ and $+C$ patched together constitute the phase-space multi valued solution in the sense of (2). We note the corresponding phase functions φ^{-Cl}, φ^{-Cr} and φ^{+C}. We can also define their respective domains Ω^{-Cl}, Ω^{-Cr} and Ω^{+C} :

$$\begin{aligned} \Omega^{-Cl} &= \{(t,x) \in [t_1, +\infty[\times\mathbb{R};\ t > \gamma^{Cr}(x)\ for\ x \geq x_1\}, \\ \Omega^{-Cr} &= \{(t,x) \in [t_1, +\infty[\times\mathbb{R};\ t > \gamma^{Cl}(x)\ for\ x \leq x_1\}, \\ \Omega^{+C} &= \Omega^{-Cl} \cap \Omega^{-Cr}, \end{aligned} \tag{33}$$

and define the PDE problems corresponding to each of these solutions :

- $-Cl$:

$$\begin{cases} \psi^{-Cl}_{,t}(t,x) + H(t,x,\psi^{-Cl}_{,x}(t,x)) = 0,\ in\ \Omega^{-Cl}, \\ \psi^{-Cl}(t_1,x) = \phi^1,\ for\ x \leq x_1, \\ (\phi^{-Cl}_{,t}, \phi^{-Cl}_{,x}).\nu = 0,\ on\ Cr, \end{cases} \tag{34}$$

- $-Cr$:

$$\begin{cases} \psi^{-Cr}_{,t}(t,x) + H(t,x,\psi^{-Cr}_{,x}(t,x)) = 0, \ in\ \Omega^{-Cr}, \\ \psi^{-Cr}(t_1,x) = \phi^1, \ for\ x \geq x_1, \\ (\phi^{-Cr}_{,t}, \phi^{-Cr}_{,x}).\nu = 0, \ on\ Cl \end{cases} \tag{35}$$

- $+C$:

$$\begin{cases} \psi^{+C}_{,t}(t,x) + H(t,x,\psi^{+C}_{,x}(t,x)) = 0, \ in\ \Omega^{+C}, \\ \psi^{+C}(t,x) = \psi^{-Cl}(t,x), \ on\ Cr, \\ \psi^{+C}(t,x) = \psi^{-Cr}(t,x), \ on\ Cl. \end{cases} \tag{36}$$

In figure 6, we plotted these different domains and indicated respectively by Γ_N or Γ_D the Neuman or Dirichlet boundaries.

Assuming the geometry of caustic cusp known, our main result is :

Theorem 5.1

$$\begin{aligned} \psi^{-Cl} &= \varphi^{-Cl}\ in\ \Omega^{-Cl}, \\ \psi^{-Cr} &= \varphi^{-Cr}\ in\ \Omega^{-Cr}, \\ \psi^{+C} &= \varphi^{+C}\ in\ \Omega^{+C}. \end{aligned} \tag{37}$$

Proof : Caustic points are conjugate points (section 2.2). Therefore, the bicharacteristics before and after these points are minima (remark 2.5). The equalities for $-Cl$ and $-Cr$ are a direct consequence of section 4.3 and identification formula (26). We recall that the bicharacteristics touch tangentially the caustic (18) and therefore satisfy the modified dynamical system of section 4.3 (i.e. satisfy normal reflection on the caustic).

For the last branch $+C$, we must check that the solution of (36), defined using the boundary data from (34) and (35), corresponds to the bicharacteristics after they reach the caustics. We proceed as in section 2.1 : the Cauchy initial data on the caustic have to match the initial conditions of system (2) restricted to the bicharacteristics issued from the caustic (i.e. the caustic is a source curve). Initial conditions on y and φ are satisfied by construction.

Concerning p, we derive a condition of type (11) from the equation and the initial condition. We remark that : i) we can use this last argument both "before" the caustic in (34) and (35) and "after" in (36). ii) We stay on the same side of the caustic. iii)Final/initial Cauchy data on the caustic are the same for (35) and (36).

The Dirichlet matching between the solutions $-C$ and $+C$ on the caustic therefore corresponds to the continuation of bicharacteristics at the caustic points. The initial condition for the bicharacteristics associated to the $+C$ branch on the caustics correspond to the restriction of the bicharacteristics "after" the caustic (proposition 2.1).

Finally we know bicharacteristics to be minima for the variational problem (8) "after" the caustic (remark 2.5). We conclude again using (26).

Remark 5.2 *We omitted to check the initial conditions of each of these problems satisfy hypothesis (12). This will always be true, for example, under the assumption of remark 2.3.*

Remark 5.3 *We used two different type of boundary conditions on the caustic. First, homogeneous Neumann conditions as obviously the Dirichlet data is not yet known. The PDE problems are well posed thanks to the remaining part of the boundary on which we have Dirichlet data. Then, for $+C$, Dirichlet data since this is known from the previous solves.*

Remark 5.4 *Problems $-C$ are 2-D Dirichlet/Neumann problems in the sense of section 4.3. Because of the shape of the domain, Dirichlet data cannot be transformed into initial Cauchy data for a time dependent equation. We explain in section 6.4 how to treat this difficulty. Conversely the last problem is a true 1-D time dependent problem. The Dirichlet data can be used as an initial Cauchy data and reciprocally.*

6 The automatic algorithm algorithm and its implementation

We explained in the previous section that *any* cusp geometric solution can be reduced to the resolution of (34), (35) and (36). We show here how this can be done without any a priori knowledge on the geometry of the caustic. This information is provided by the transport equation (30) coupled to the Hamilton-Jacobi equation.

6.1 The single valued part

Smooth initial data ϕ^0 is prescribed on $t = t_0$ (Γ). We solve the coupled system (21)-(30) (initial conditions for (30) can be computed from (11)). We do so until we *detect* a point (t_1, x_1) such that $D(t_1, x_1) = \delta(t_1, x_1)[1] = 0$ (figure 2). This is a cusp vertex and we have reached time when the smooth solution becomes singular. We call (ϕ^1, δ^1) the solution on this line $t = t_1$ and stop. Should we continue to march in time, the viscosity solution would develop a kink as mentioned in section 5.2 (figure 4).

6.2 The $-C$ branches : a free boundary problem

We only describe this step for the $-Cl$ branch ($-Cr$ can be deduced by symmetry). We have to solve (34) with an additional difficulty : we do not know the shape of Cr. To do so,

we define the *free boundary problem* :

$$\begin{cases} \psi^{-Cl}_{,t}(t,x) + H(t,x,\psi^{-Cl}_{,x}(t,x)) = 0, \ and \\ \delta^{-Cl}_{,t}(t,x) + H_{,p}(t,x,\psi^{-Cl}_{,x})\delta^{-Cl}_{,x}(t,x) = A(t,x,\psi^{-Cl}_{,x}(x)).\delta^{-Cl}(t,x), ... \\ in\ \Omega^{FB}(\psi^{-Cl},\delta^{-Cl}), \\ \psi^{-Cl}(t_1,x) = \phi^1, \ and \\ \delta^{-Cl}(t_1,x) = \delta^1(t_1,x), \ for\ x \leq x_1, \end{cases} \tag{38}$$

where the domain depends on the solution by the intermediate the associated D function (see section 4.4). If D is positive on $t = t_1$, we have:

$$\Omega^{FB}(\psi^{-Cl},\delta^{-Cl}) = \{(t,x) \in]t^1, +\infty[\times\mathbb{R};\ D(t,x) > 0\}. \tag{39}$$

We know that D vanishes and change its sign when a bicharacteristics reach the caustic tangentially (18). It is in particular the case at point (t_1, x_1) and at all the points on Cr. The solution of problem (38) therefore satisfies :

$$\Omega^{FB}(\psi^{-Cl},\delta^{-Cl}) = \Omega^{-Cl}.$$

We further know (still (18)) that the trace of the normal derivative (in (t,x) space of the phase function on the caustic satisfies :

$$(\phi^{-Cl}_{,t}, \phi^{-Cl}_{,x}).\nu = 0, \ on\ Cr.$$

Therefore, *problem (38) is equivalent to (34).* We detail the numerical strategy for solving (38) in section 6.4.

Remark 6.1 *The bicharacteristic interpretation of section 4.2 and 4.3 holds for the free boundary problem. We use here the a priori knowledge on the structure of the solution $-Cl$ which predicts that bicharacteristics are minima precisely up to the free boundary.*

6.3 The $+C$ branch

Once the $-C$ solution is known on the caustic (Cl and Cr) we can simply use equation (36). We can again couple this equation to transport equation (30). In this case the initial conditions for δ can be given by the $-C$ branch (but in any case correspond to (18)).

6.4 1-D treatment of the free boundary problem

As discussed in section 4.3 and remark 4.4 problem (38) is a 2-D problem because : i) the free boundary (corresponding to Cr) is not known a priori; ii) even if we knew the geometry of Cr, we do not know the value of the solution on this curve and therefore can not use it

as Cauchy initial data for the time dependent problem.

When the tangents to the caustic have maximal angle of 45^o and minimal angle of 0^o with the t axis, we propose the simple numerical procedure :

Let (ϕ_i^n, δ_i^n) be a discrete numerical approximation at points $(n*dt, i*dx)$ discretizing the domain. At time step n, the solution is given for $i \leq i_c$, i_c is the space index of the caustic. We then compute the upwind viscosity solution $(\phi_i^{n+1}, \delta_i^{n+1})$ still for $i \leq i_c$. Remark this part of the solution is correct because the bicharacteristics point right-wise. We now distinguish two cases (figure 7). Either $\delta_{i_c}^{n+1}[1] = 0$ in which case i_c remains the index of the caustic (figure 7 a)); or $\delta_{i_c}^{n+1}[1] \neq 0$ (figure 7 b)). In this last situation we proceed as follow :

- We assume the caustic makes a 45^o angle with t axis therefore linking points $(n*dt, i_c*dx)$ and $((n+1)*dt, (i_c+1)*dx)$ (the discretization must satisfy $dx = dt$).
- As homogeneous Neumann boundary condition are satisfied by ψ^{-Cl} on the caustic (34), $\phi_{i_c+1}^n = \phi_{i_c}^{n+1}$ is a reasonable approximation (figure 7 b)).
- We march in time, starting again at $n*dt$ but for $i \leq ic+1$. We obtain the solution $\phi_{i_c+1}^{n+1}$ at the new caustic index i_c+1.
- We set $\delta_{i_c+1}^{n+1} = (0,0)^T$ on the caustic (18) and iterate the process.

The question of accuracy and consistency of this process has not been investigated (it approximates the caustic using vertical and 45^o slope segments). Its implementation gives satisfactory numerical results (section 8). It could also be adapted to treat more general caustics.

Another possibility to solve the free boundary problem is to use upwind derivative $d\phi_{i_c}^- = \frac{\phi_{i_c}^n - \phi_{i_c-1}^n}{dx}$. It approximates the slope of the caustic. Caustic position at time level $(n+1)*dt$ should be $i_c^{n+1} = i_c^n + dt * d\phi_{i_c}^-$. We can define the missing values $(\phi_i^{n+1}, \delta_i^{n+1})$ for $i_c^n < i < i_c^{n+1}$ using various (interpolation or bicharacteristic) techniques. One can also decide to use variable steps dx to improve the discretization of the caustic curve.

6.5 The algorithm for multiple cusps

The previous sections explain how to deal with a simple cusp. For more complicated situations such as described in section 3.4, we need to define a strategy. For two cusps we first distinguish between case a) b) and c) of figure 3. Case a) and case b) are identical from the algorithmic point of view :

- Once one of the cusp vertex is detected, we apply the strategy of section 6.2-6.3. This generates three branches associated to the first cusp. Let us call them : ψ_1^{-Cl}, ψ_1^{-Cr} and ψ_1^{+C}.

- The same strategy is applied to each of the lateral branch ψ_1^{-Cl} and ψ_1^{-Cr}. If a second cusp appear say in the left branch, it bifurcates into three new branches noted ψ_2^{-Cl}, ψ_2^{-Cr} and ψ_2^{+C}.
- Branches ψ_1^{-Cl} and ψ_2^{-Cr} actually merge and are restricted to $\Omega_1^{-Cl} \cap \Omega_2^{-Cr}$ (using the domains definition (33)) :

$$\psi_1^{-Cl} = \psi_2^{-Cr}, \ on \ \Omega_1^{-Cl} \cap \Omega_2^{-Cr}.$$

  We recover 5 different branches on the overlap of the cusps when it is not empty. The right case is dealt with identically. If the second cusp arise at the same time as the first one, the procedure is unchanged.

Case c) is different :

- Same start as first point above.
- We then look for a cusp vertex appearing in the ψ_1^{+C} branch and simply apply the same (section 6.2-6.3) strategy. It gives a second cusp solution again noted ψ_2^{-Cl}, ψ_2^{-Cr} and ψ_2^{+C}.
- Since the apparition of the second cusp, the ψ_1^{+C} branch bifurcates into the two $-C$ branches ψ_2^{-Cl} and ψ_2^{-Cr}. We eliminate ψ_1^{+C} and ψ_2^{-Cl} and ψ_2^{-Cr} are respectively supported in $\Omega_1^{+C} \cap \Omega_2^{-Cl}$ and $\Omega_1^{+C} \cap \Omega_2^{-Cr}$ and again get 5 branches.

When more than two cusps interact (i.e. more than 5 branches) A recursive treatment of all branches should be possible according to their $\pm C$ type and following these two strategies.

7 Generalizations

7.1 Generalization to 2-D Hamilton-Jacobi equations

The results of section 2 and 4 also hold in higher dimensions. The generic classification of singularities (section 3) gets more complicated : the number of possible cases increases (3 in 2-D) and caustics are surfaces. Definition (3) generalizes to :

$$D(y(s,x^0)) = dy_1 \wedge dy_2 \wedge ds = det(\frac{\partial y_i(s,x^0)}{\partial x_j^0}) dx_1^0 \wedge dx_2^0 \wedge ds.$$

This Jacobian matrix carries information on the type of singularity encountered and is computed by the transport equation. We believe it is possible to work out a splitting similar to the one carried out in section 5 for each type of singularity. Then one should carefully study the possible interaction of these singularities to check that an automatic adaptative algorithm can be implemented. The resolution of the Hamilton-Jacobi equation and the transport equation in higher dimensions is possible [Em96].

7.2 Application to scalar conservation laws

In 1-D, it is well known that it suffices to derive (1) and set $u = \phi_{,x}$ to recover the scalar conservation law :

$$\begin{cases} u_{,t}(t,x) + H_{,p}(t,x,u(t,x)) = 0, \ in\ \Omega = \{(t,x) \in \mathbb{R} \times \mathbb{R},\ t > \gamma(x)\} \\ u(\gamma(x),x) = \phi^0_{,x}(x),\ for\ x \in \mathbb{R}. \end{cases}$$

We recover for instance Burgers equation from the Eikonal equation with homogeneous slowness index. Under this transformation, the algorithm presented solves the same multi valued phase-space problem (as can be seen from line b) of figure 2. The outgoing boundary condition (section 4.5) can be used to truncate the solution at caustic points. The infinite (or large) Dirichlet condition is interpreted as the extension of the solution using a steep slope at caustic points. A discrete time marching scheme using such an extension should be very accurate in recovering the smooth solution. We can also think of detecting shocks from the multi valued solution (in the spirit of [Bre84]).

7.3 Reflections

It is interesting to note that the same patching technique can be used to treat reflection of bicharacteristics on a fixed boundary. The reflection can be symmetrical with respect to the normal (as for caustics) but may also obey more sophisticated reflection laws (see Theorem 5.10 in [Bar94]). This technique was originally proposed in [EFO95] for geometrical optics (normal reflection). Note however that the introduction of such boundaries may generate new types of singularity and complicate somewhat the generic classification [Izu].

7.4 Shock and caustic detection : an algorithmic classification of branches

The other possibility to split the multi valued solution in the case of the cusp for example is :

- First compute the global viscosity solution (in Ω).
- Detect the kink (shock) using an ad-hoc algorithm.
- Generate a new solution from the kink using it as source curve.
- Finish the computation by patching the solution at the caustic as proposed in section 5.

The first three points of this program are proposed in [EFO95]. The full procedure is more complicated and more delicate to implement (kink detection is not always robust) than the algorithm of section 5. It leads however to an interesting *conjecture* for stationary Hamilton-Jacobi equations :

Any multi valued solution for such problems can possibly be recovered iteratively by successive viscosity solutions using the following strategy :

- Initialize the process by computing the viscosity solution in all the domain.
- Detect all kinks and caustics. For caustics use the transport equation as in the free boundary problem (38).
- Use the trace of the solution as boundary condition on kinks and caustics for a new iteration. In the case of shocks these condition are isotropic. For caustic, we must restrict the domain of resolution to the side of the previous solution.
- Go back to the second point and iterate until no kinks and caustics are detected.

The interested reader can convince himself that this algorithm works on simple examples involving one or two cusps (see also [BKB]). We think that this algorithm moreover satisfy the following nice ordering property :
Let (ϕ^k) be the successive solutions, k being the iteration index. They are not necessary all supported in the full domain Ω. We adopt the convention that, wherever a function ϕ^k is not defined, it takes the value of its "parent" (ϕ^{k-1}) (this rule can, of course, be applied recursively). Then :

$$\textit{For } k_1 \leq k_2 \leq ... \leq k_n \textit{ we have}$$
$$\phi^{k_1}(x) \leq \phi^{k_2}(x) \leq ... \leq \phi^{k_n}(x), \forall x \in \Omega.$$

8 Application to geometrical optics

8.1 The 2-D problem

We restrict to a particular form of stationary Hamilton-Jacobi equation and refer to the introduction and the references therein for a discussion on the underlying motivations. The Eikonal equation can be written :

$$\frac{1}{2}(\phi^2_{,x_1}(x_1,x_2) + \phi^2_{,x_2}(x_1,x_2) - n^2(x_1,x_2)) = 0,\ (x_1,x_2) \in \mathbb{R}^- \times \mathbb{R}, \tag{40}$$

where $n = \frac{1}{c}$ is the slowness index (c is a smooth (C^2) strictly positive function modeling wave velocity in the medium). We add for simplicity a source boundary condition on $x_1 = 0$:

$$\phi(0,x_2) = \phi^0(x_2),\ x_2 \in \mathbb{R}. \tag{41}$$

Point or parameterized curve source conditions can also be considered.

In this case, the 2-D Hamiltonian is $H(x_1,x_2,p_1,p_2) = \frac{1}{2}(p_1^2 + p_2^2 - n^2(x_1,x_2))$ and has many equivalent forms. The corresponding Hamiltonian system is still (2) (y and p are vectors) and the time parameterization of these ODEs depends on the particular choice of

the Hamiltonian. Bicharacteristic curves are called *rays* and the contour lines of the phase, normal to rays, *fronts*. We also have locally :

$$\dot{y}(s,x^0) = p(s,x^0) = (\phi_{,x_1}(y(s,x^0)), \phi_{,x_2}(y(s,x^0))). \tag{42}$$

8.2 A paraxial restriction on rays

It is possible to greatly simplify this problem under the assumption :

$$\phi_{,x_1} < 0.$$

According to (42), it means that rays/bicharacteristics only propagate in the $x_1 < 0$ direction. In this case (40) can be reduced to :

$$\phi_{,x_1}(x_1,x_2) + \sqrt{\phi^2_{,x_2}(x_1,x_2) - n^2(x_1,x_2)} = 0,\ (x_1,x_2) \in \mathbb{R}^+ \times \mathbb{R}. \tag{43}$$

We recognize a 1-D time dependent problem. It exactly fits the framework of (1) (with (41)). We can therefore apply our method to the particular Hamiltonian :

$$H(x_1,x_2,p_2) = \sqrt{p_2^2 - n^2(x_1,x_2)}.$$

where x_1 stands for the time variable $-t$ and x_2 for x. This function satisfy all the assumptions on H (including remark 2.3).

This approach has been extensively studied in [SVST94] [SS94] [Em96] for 2-D and 3-D problems. A truncation technique has been developed to eliminate potential turning rays and an adaptative Runge-Kutta method is used for time accuracy. We use a 1-D matlab implementation of this algorithm.

8.3 Numerical test

Our test problem corresponds to case c) of figure 3. We programmed the *automatic* detection and generation of the two successive cusps in matlab following the strategy described in section 6.5.

The velocity profile c is analytically given by (figure 8) :

$$c(t,x) = 1 + 0.2 * sin(\pi * 0.5 * t). * sin(\pi * 3 * x),\ for (t,x) \in [0,3] \times [0,1].$$

The corresponding bicharacteristic curves $y(.,x^0)$ are represented in figure 9). They correspond to a point source condition :

$$\begin{cases} y(0,\theta) = (0, 0.55), \\ p(0,\theta) = n(0,0.55) * (cos(\theta), sin(\theta)), \\ \varphi(0,\theta) = \phi^0(x^0),\ for\ \theta \in [0.3*\pi, 0.7*\pi]. \end{cases}$$

Here θ is the initial "shooting" angle of each ray. One can recover equivalent initial conditions (in the form (2)) on $t = dt$ (after one time step) using a ray approximation. Note that there is no symmetry in the solution. Rays form two envelopes corresponding to the cusped caustics.

Figure 10 represent the solution for the first cusp, i.e. the solutions $(\psi_1^{-Cl}, \delta_1^{-Cl}[1])$ $(\psi_1^{-Cr}, \delta_1^{-Cr}[1])$ and $(\psi_1^{+C}, \delta_1^{+C}[1])$ (see section 6.4 and 6.5). We display on the left the contour lines of the phase (sampled every $0.01s$.) and on the right, a color map of the value of D. The fronts are correct and correspond to the generic splitting of figure 5. A kink is distinguishable in the $+C$ branch. It actually bifurcates to generate a new cusp. The determinant of the Jacobian D, simply $\delta_1^{\pm C}[1]$ in this case, is negative for the $-C$ branches, 0 on the caustic and positive for the $+C$ branches. We recover correctly the free boundary and the position of the second cusp vertex (a white spot) is detected.

Figure 11 represents the solution for the second cusp, i.e. the solutions $(\psi_1^{-Cl}, \delta_2^{-Cl}[1])$ $(\psi_2^{-Cr}, \delta_2^{-Cr}[1])$ and $(\psi_2^{+C}, \delta_2^{+C}[1])$.

We aggregated all fronts in figure 12. One can clearly see the two cusps developing along time. In order to check the accuracy of our method we compared with a result obtained using a *two point ray tracing method* [KKC94]. It is an iterative method (computationally expensive) able to find all rays between two prescribed points. We compare the *time traces* at $t = 2.5$. It means that we plot the value of the multi valued phase function $\phi(1.8, x)$ for $x \in [0.1]$. On the left of figure 13 is our solution and on the right the two point ray tracing obtained on a coarser mesh. The two are in good accordance.

8.4 Link with Keller-Maslov theory

There is a methodological link with this theory. Roughly speaking, Maslov use the generic classification of singularity to evaluate oscillatory integrals near caustics. These oscillatory integrals arise as ansatz of solutions for high frequency asymptotic solution of the wave and Schrödinger equation. For more on these topics, see [Dui74].

The geometrical theory of diffraction [Kel58] [Lud66] gives the same approximation of the reduced wave equation near cusped caustics. The decomposition of the solution in a neighborhood of the caustic actually corresponds to section 5. The main difficulty in classical geometrical optics is the computation of the amplitude of the high frequency asymptotic solution. The "classical" amplitude is proportional to $\frac{1}{\sqrt{D}}$ and blows up at caustics. Based on the decomposition of the phase function, geometrical theory of diffraction provides modified transport equations for the amplitudes which remain valid near caustics. Our method computes all needed quantities to solve these modified transport equations. It should therefore be possible to get the correct amplitudes near caustics (more details in [Ben97]).

9 Conclusion

We hope that the reader which has reached this point is convinced that it is possible to automatically perform phase-space ($\mathbb{R}_y \times \mathbb{R}_p$) computations only in position space $\mathbb{R}_y$. We did not try to obtain the weakest assumptions under which the presented results hold, but instead chose to set the problem in such a way that the combination of the different used theories work.

We finish by listing the advantages and disadvantages we see to this method. We want to emphasize two of the nice feature of the algorithm :

It splits the multi-valued solution into smooth single valued solution. These solutions can not only be computed by upwind schemes but also are easy to compute because they are smooth (no kinks). This algorithm is optimal in term of computational cost. Whatever the scheme used, we are guaranteed to discretize and work exactly on the projection of the support of the solution in phase-space. The transport equation penalizes the cost. However, for geometrical optics for instance, this equation has a physical meaning and its solution is a sought for quantity.

The main difficulty is the the implementation. Relatively simple in 1-D, the automatic detection of caustics and the sorting and patching of different branches is possible but certainly difficult in 2-D.

Aknowledgements

We wish here to express our gratitude to : F. Collino, G. Kossioris, A.P.E. Ten Kroode and S. Izumiya for their precious help on the Differential geometry approach of the problem. R. Abgrall and G. Barles for kindly answering our naive questions on viscosity solutions. Y. Brenier for his remarks on the application of this method to scalar conservation laws (section 7.2). W.W. Symes for providing the 1-D matlab Eikonal solver used in this paper as a building block of the general algorithm and for his wise advice. Discussions with L. Klimes on geometrical optics have been particularly useful. He also computed the reference solution of the test problem. Finally, we thank R. Martin for his efficient realization of figures 1 to 6.

References

[Abg96] R. Abgrall. Numerical Discretization of First Order Hamilton Jacobi Equations on Triangular Meshes. *Comm. in Pure and Applied Math.*, 1996.

[AGZV86] V. I. Arnol'd, S.M. Gusein-Zade, and A.N. Varchenko. *Singularities of Differential Maps.* Birkhauser, 1986.

[Arn92] V. I. Arnol'd. *Catastrophe theory.* Springer-Verlag, 1992.

[Bar94] G. Barles. *Solutions de viscosité des équations de Hamilton-Jacobi.* Springer-Verlag, 1994.

[Ben96] J.-D. Benamou. Big ray tracing : Multivalued travel time field computation using viscosity solutions of the eikonal equation. *J. Comp. Physics*, 128:463–474, 1996.

[Ben97] J.-D. Benamou. Multivalued solution and viscosity solution of the eikonal equation. *INRIA tech. report 3281*, 1997.

[Bey85] G. Beylkin. Imaging of discontinuities in the inverse scattering problem by inversion of a causal generalized radon transform. *Journal of Mathematical Physics*, 26:99–108, 1985.

[BG85] N. Bleistein and S. H. Gray. An extension of the born inversion method to a depth dependent reference profile. *Geophysical Prospecting*, 33:999–1022, 1985.

[BKB] J.-D. Benamou, L. Klimes, and P. Bulant. Phase space decomposition of the multi-valued travel-time field using shocks and caustics. *in preparation.*

[BL96] Y. Brenier and L.Corrias. A kinetic formulation for multi-branch entropy solutions of scalar conservation laws. *Ann. IHP Analyse non-linéaire*, 1996.

[Bre84] Y. Brenier. Averaged multivalued solutions for scalar conservation laws. *SIAM J. Numer. Anal.*, 21:1013–1037, 1984.

[CL83] M.G. Crandall and P.L. Lions. Viscosity solutions of hamilton-jacobi equations. *Trans. Amer. Math. Soc.*, 277:1–42, 1983.

[Dui74] J.J. Duistermaat. Oscillatory integrals, lagrange immersions and unfolding of singularities. *Comm. Pure Appl. Math.*, 27:207–281, 1974.

[EFO] B. Engquist, E. Fatemi, and S. Osher. Finite difference methods for geometrical optics and related nonlinear pdes approximating the high frequency helmholtz equation. *CAM report 90024-1555, UCLA.*

[EFO95] B. Engquist, E. Fatemi, and S. Osher. Numerical resolution of the high frequency asymptotic expansion of the scalar wave equation. *J. Comp. Physics*, 120:145–155, 1995.

[Em96] M. Abd El-magged. 3-d first arrival traveltimes and amplitudes via eikonal and transport finite difference solvers. *Rice University thesis*, 1996.

[ER95] B. Engquist and O. Runborg. Multi-phase computation in geometrical optics. *Tech report, Nada KTH*, 1995.

[FS93] W. H. Fleming and H. M. Soner. *Controlled Markov Processes and Viscosity Solutions*. Springer-Verlag, 1993.

[GB93] S. Geoltrain and J. Brac. Can we image complex structures with first-arrival traveltime ? *Geophysics*, 58:564–575, 1993.

[GF63] I.M. Gelfand and S.V Fomin. *Calculus of Variation*. Prentice-Hall, 1963.

[IK] S. Izumiya and G. Kossioris. Bifurcation of shock waves for viscosity solutions of hamilton-jacobi equations of one space variable. *Bull. Sci. Math.*

[Izu] S. Izumiya. Singularities of multi valued solution of first order pdes. *Communication at the workshop on 'hyperbolic aspect of moment closure problems' (Heraklio, april 98)*.

[Izu93] S. Izumiya. The theory of legendrian unfoldings and first order differential equations. *Proc. Royal Soc. Edinburgh*, 123A:517–532, 1993.

[Kel58] J.B. Keller. A geometrical theory of diffraction. In *Calculus of variations and its applications Vol, 8*. McGraw-Hill, New-York, 1958.

[KKC94] L. Klimes, M. Kvasnicka, and V. Cerveny. Grid computations of rays and travel times. in : Seismic waves in complex 3-d structures, report 1. *Tech. Report, Department of Geophysics, Charles University Prague*, pages 85–114, 1994.

[KSV] A.P.E. Ten Kroode, D.J. Smit, and A.R. Verdel. A microlocal analysis of migration. *Wave Motion*.

[LLH96] G. Lambare, P. Lucio, and A. Hanyga. Two dimensional multivalued traveltime and amplitude maps by uniform sampling of a ray field. *Geophys. J. Int*, 125:584–598, 1996.

[Lud66] D. Ludwig. Uniform asymptotic expansions at a caustic. *Comm. Pure Appl. Math.*, 19:215–250, 1966.

[OS89] S. J. Osher and C.W. Shu. High-order essentially nonoscillatory schemes for hamilton-jacobi equations. *SIAM J. Numer. Anal.*, 83:32–78, 1989.

[per]

[RT88] E. Rouy. and A. Tourin. A viscosity solution approach to shape-from-shading. *SIAM J. Numer. Anal.*, 29:867–884, 1988.

[Set96] J. Sethian. *Level set methods*. Cambridge university press, 1996.

[Son86] H. M. Soner. Optimal control problems with state space constraints. *SIAM J. Control and optim.*, 24:552–561, 1986.

[SS94] A. Sei and W. Symes. Gradient calculation of the traveltime cost function without ray tracing. In *Proceedings of the 64th SEG annual meeting*, 1994.

[SVST94] W. Symes, R. Versteeg, A. Sei, and Q. H. Tran. Kirchhoff simulation migration and inversion using finite-difference traveltimes and amplitudes. *TRIP tech. Report, Rice U.*, 1994.

[Sym96] W. Symes. A slowness matching algorithm for multiple traveltimes. *preprint*, 1996.

[TS91] J. Van Trier and W. W. Symes. Upwind finite-difference calculation of traveltimes. *Geophysics*, 56:812–821, 1991.

[Vid88] J. Vidale. Finite-difference calculation of traveltimes. *Bull. Seis. Soc. Am.*, 78:2062–2076, 1988.

[VIG93] V. Vinje, E. Iversen, and H. Gjoystdal. Traveltime and amplitude estimation using wavefront construction. *Geophysics*, 58:1157–1166, 1993.

[You69] L.C. Young. *Lecture on the Calculus of Variation and Optimal Control Theory.* 1969.

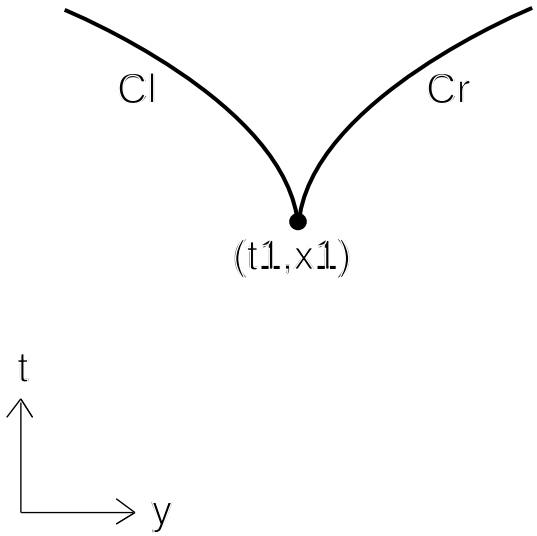

Figure 1: Cusp (A_3 singularity)

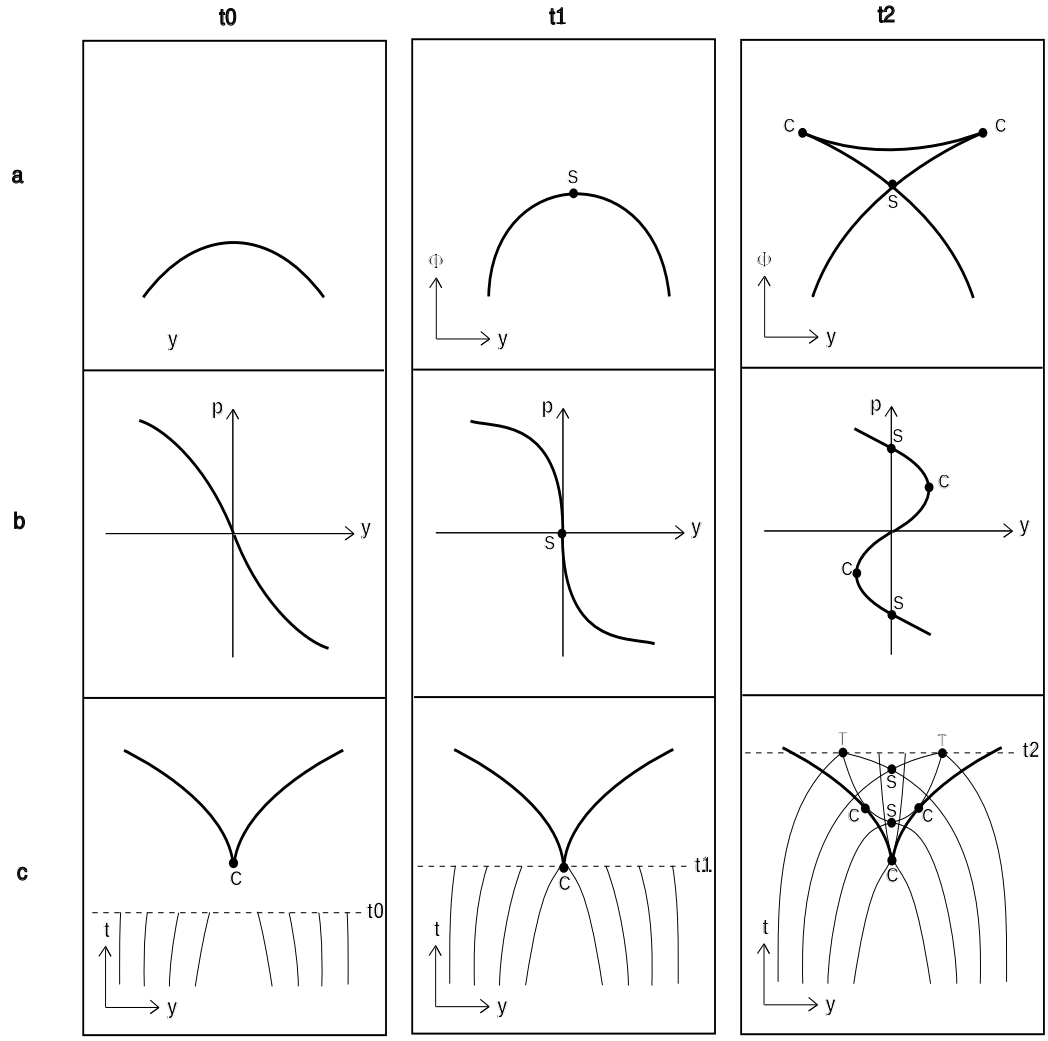

Figure 2: Time evolution of the geometric solution

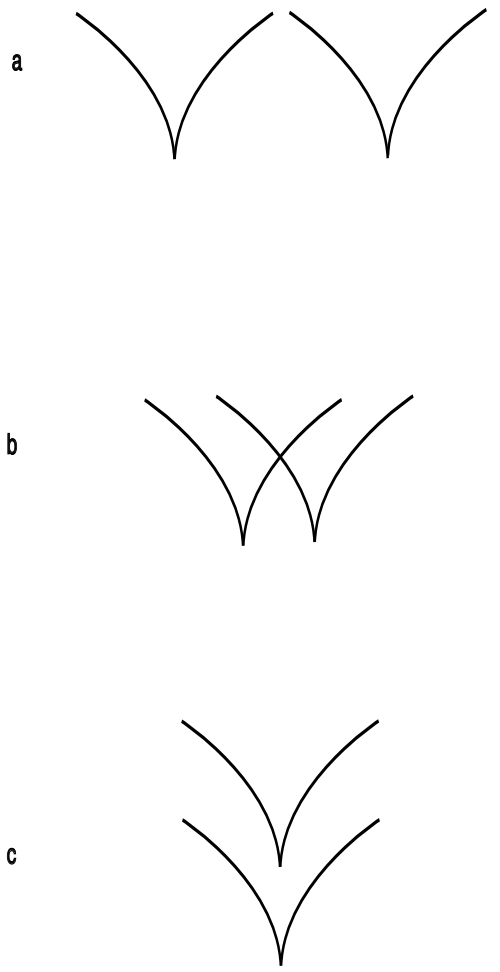

Figure 3: Cusps interactions

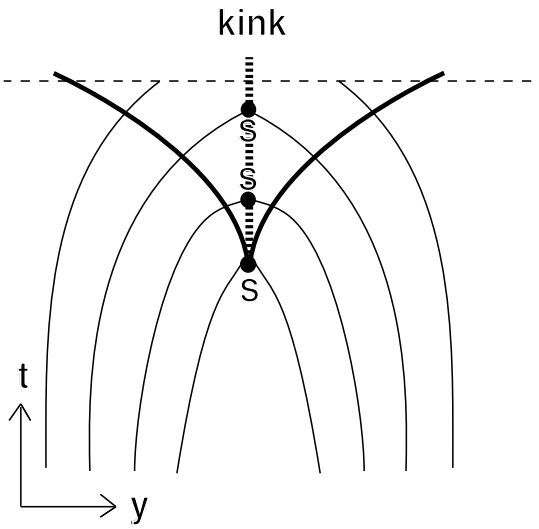

Figure 4: Singular solution (with kink)

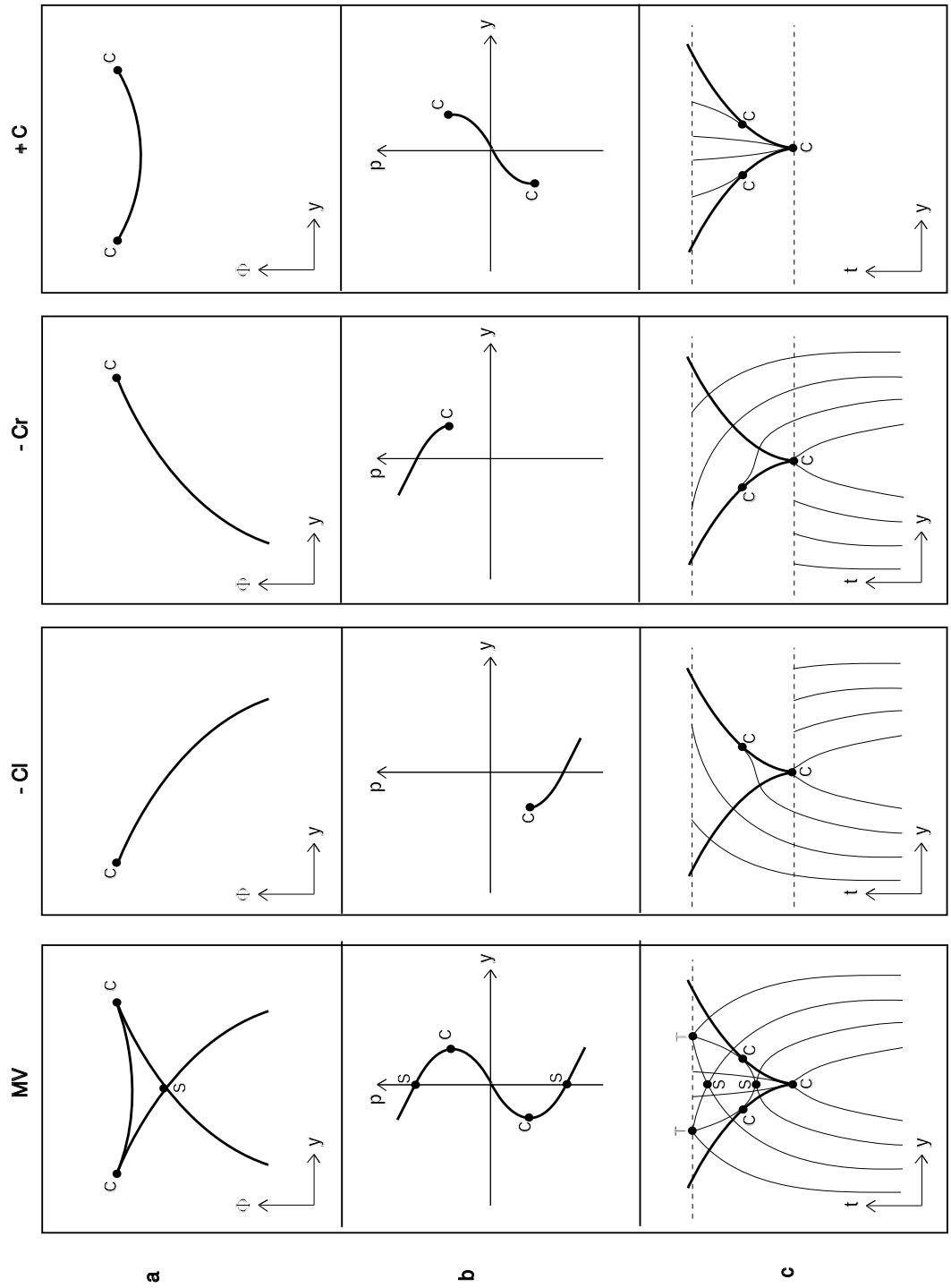

Figure 5: Spliting of the multi valued solution

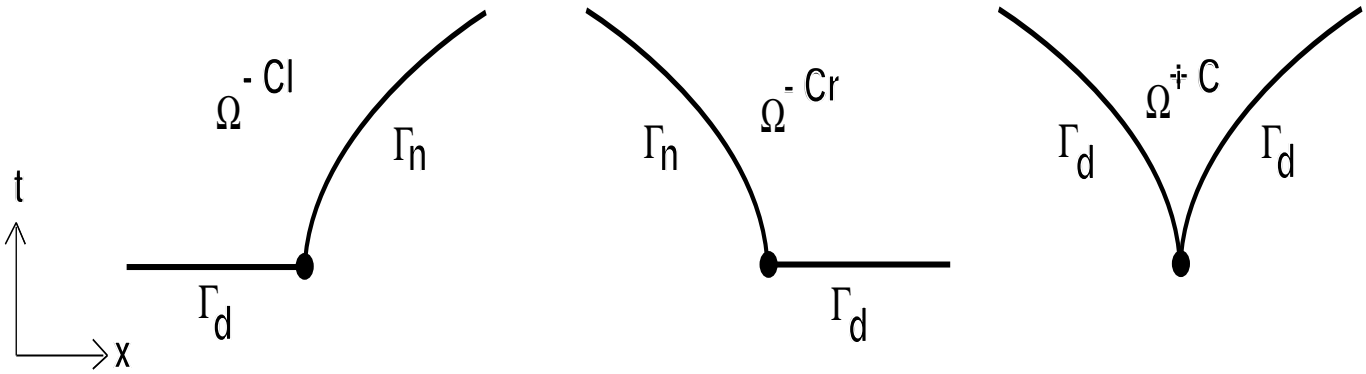

Figure 6: Domains of definition of the branches $\pm C$

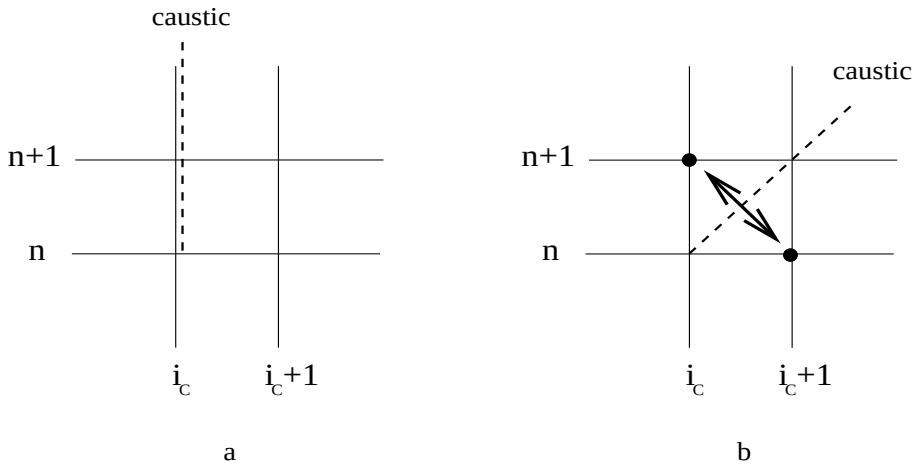

Figure 7: Free boundary detection

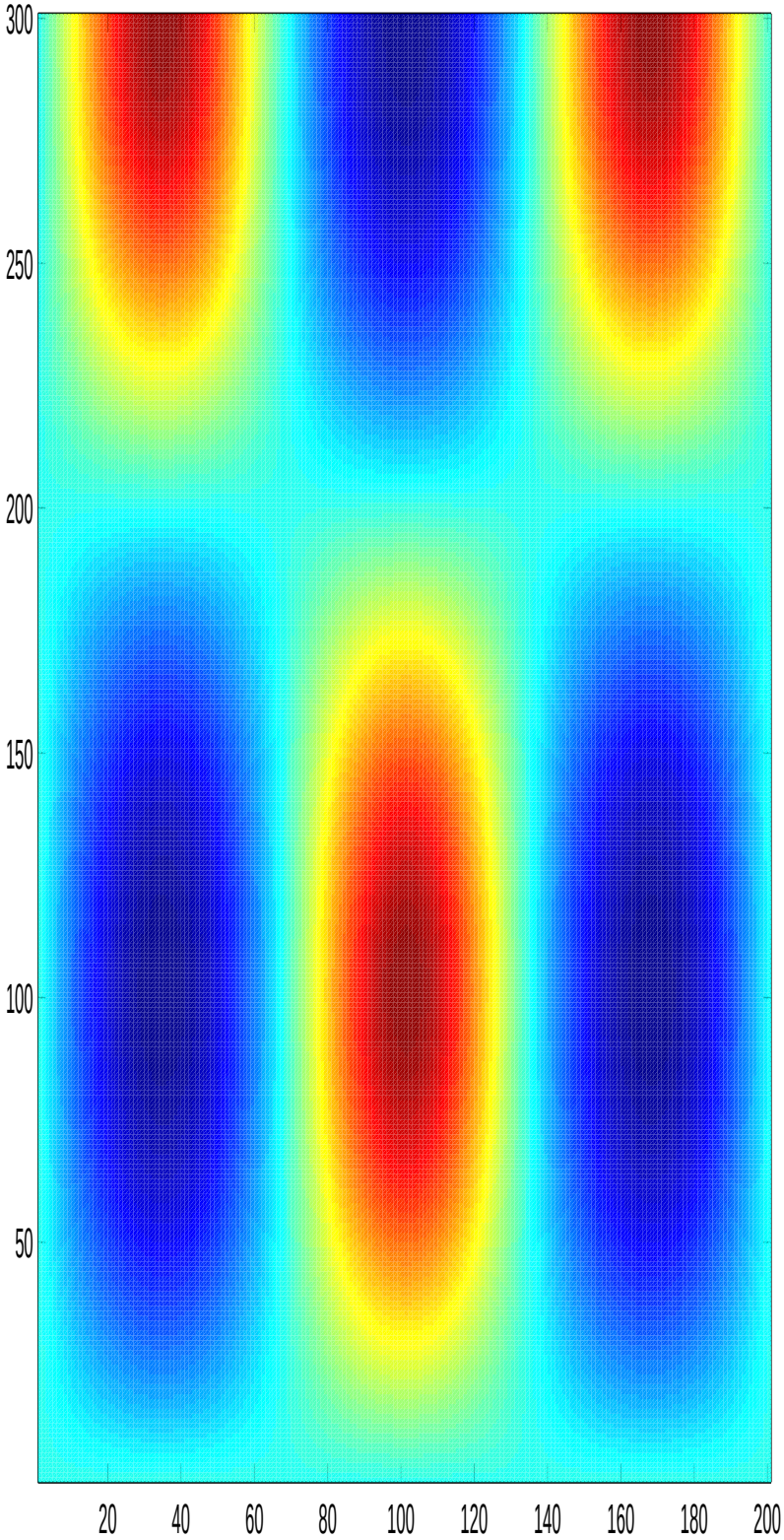

Figure 8: Speed c $(= \frac{1}{7}n)$

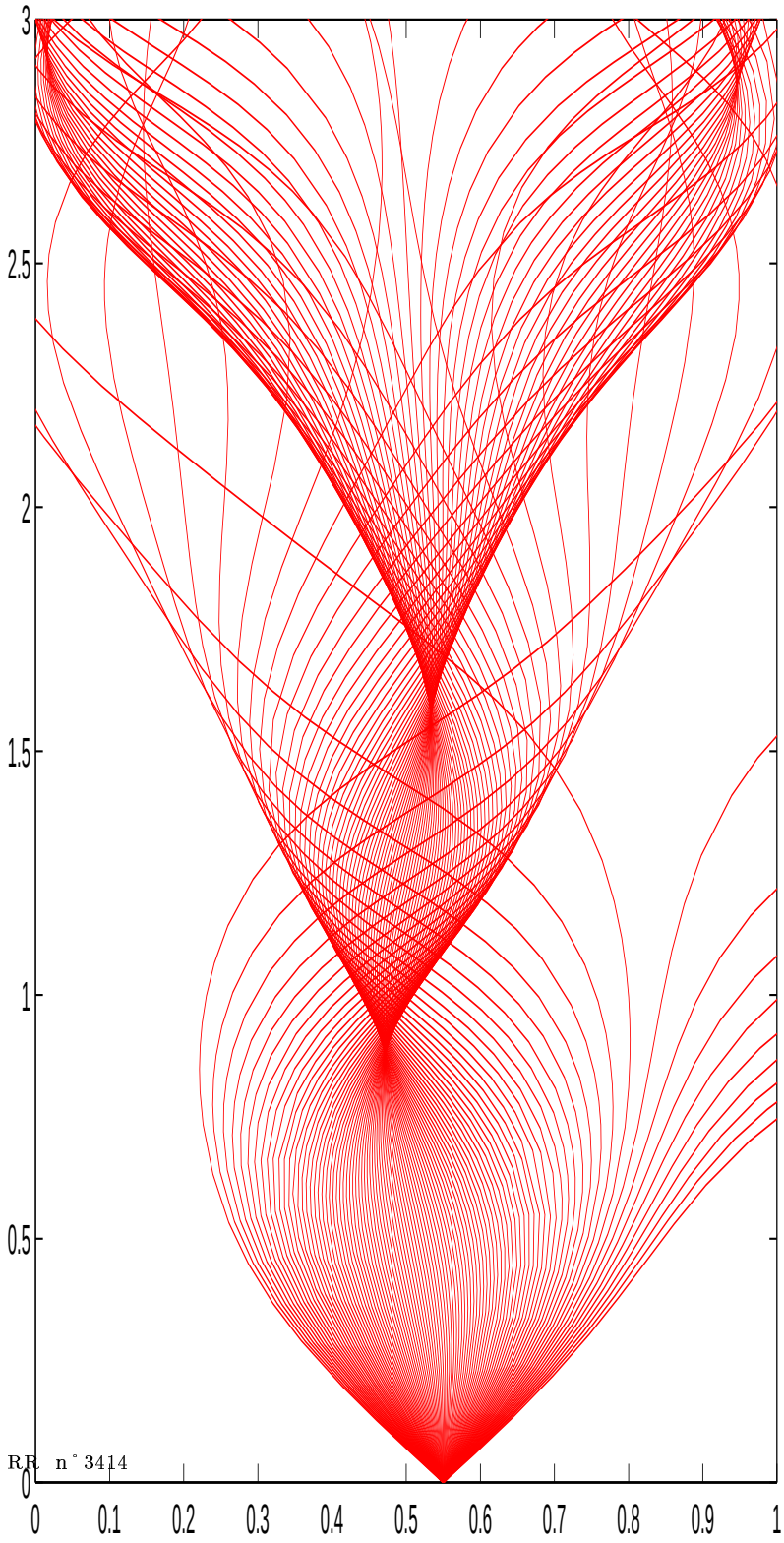

Figure 9: Bicharacteristics curves (t is the vertical axis)

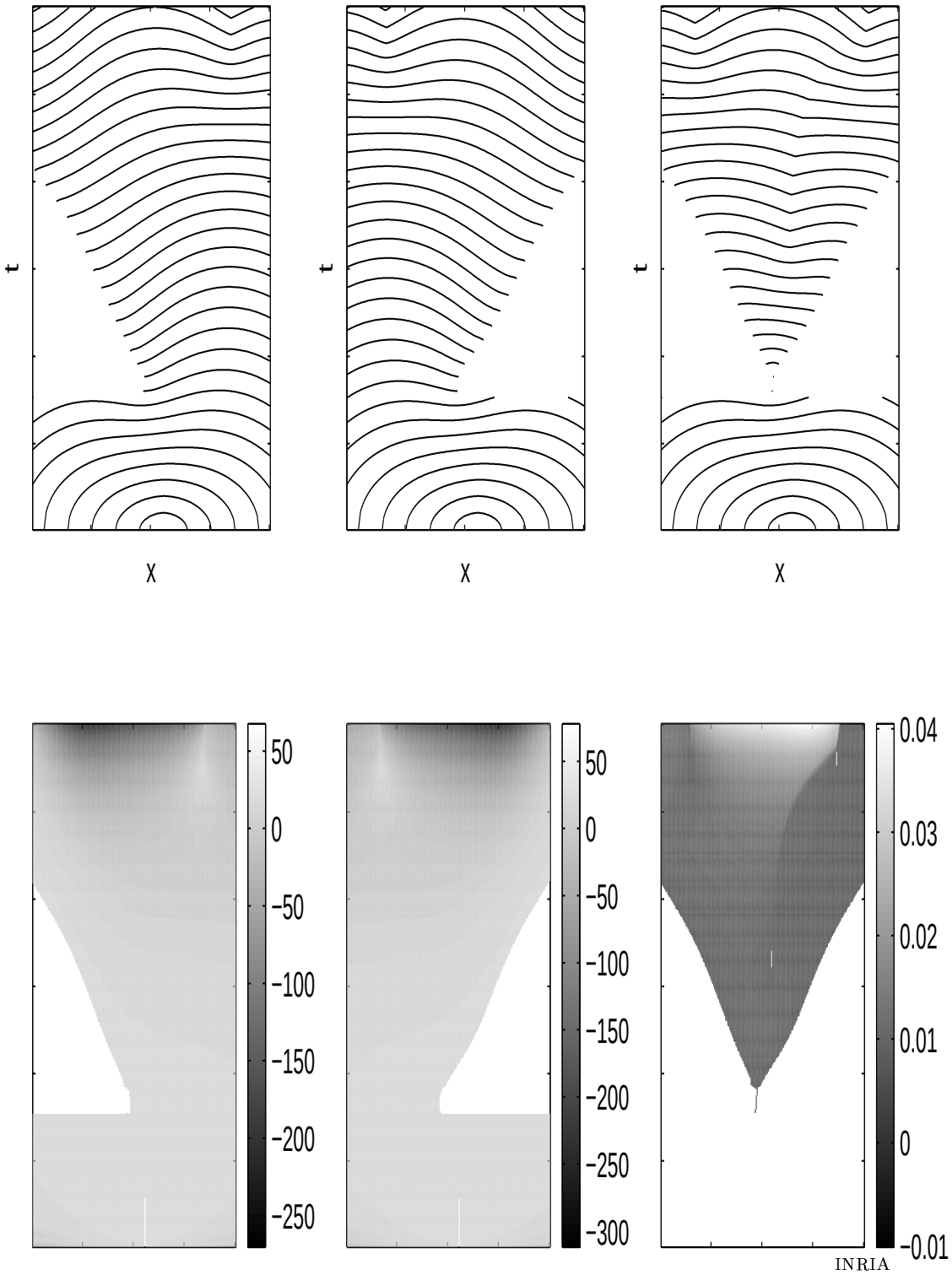

Figure 10: First cusp. Left : contour lines of $\psi^{\pm C}$. Right D $(= \delta^{-Cl}[1])$

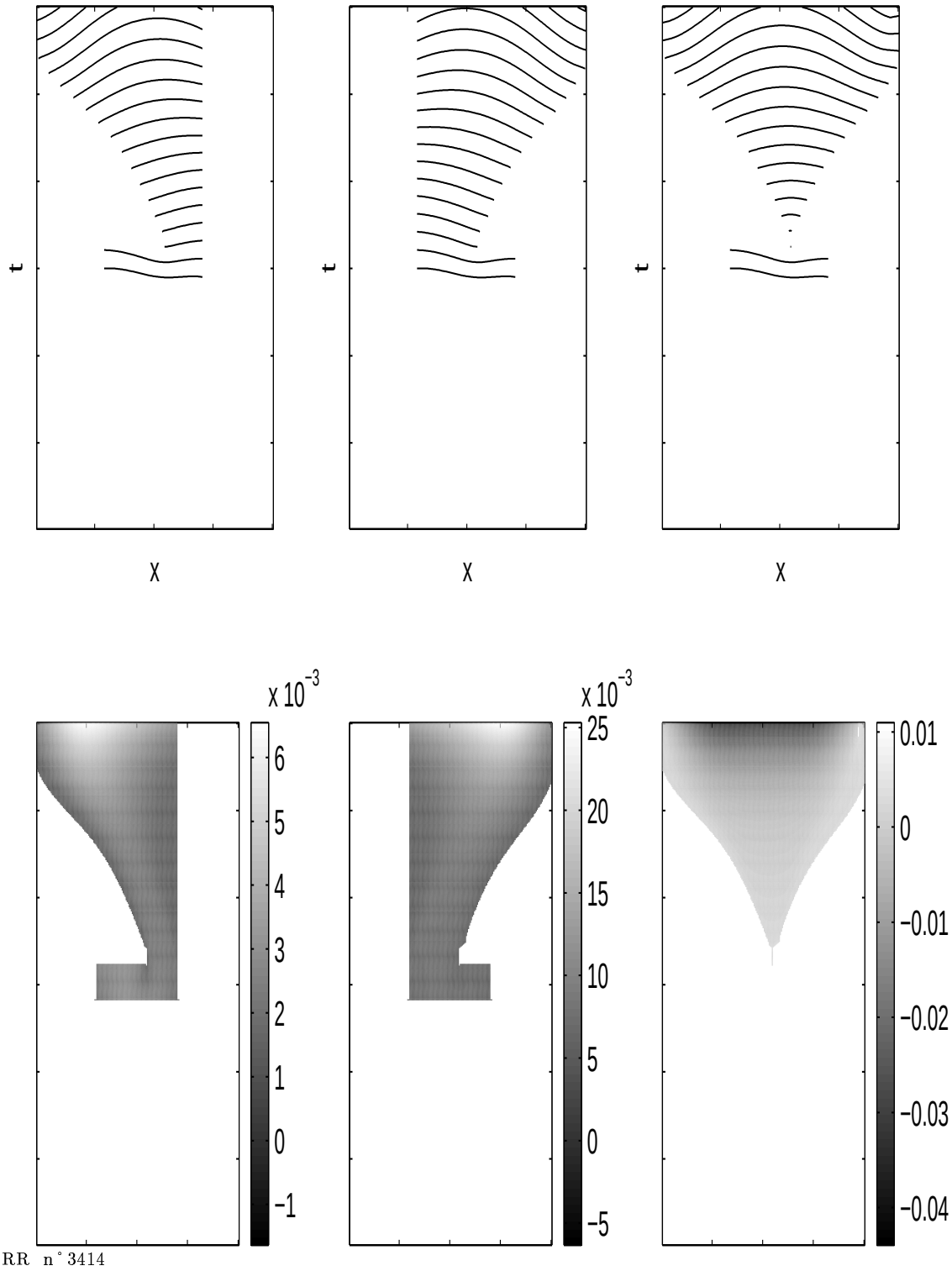

Figure 11: Second cusp

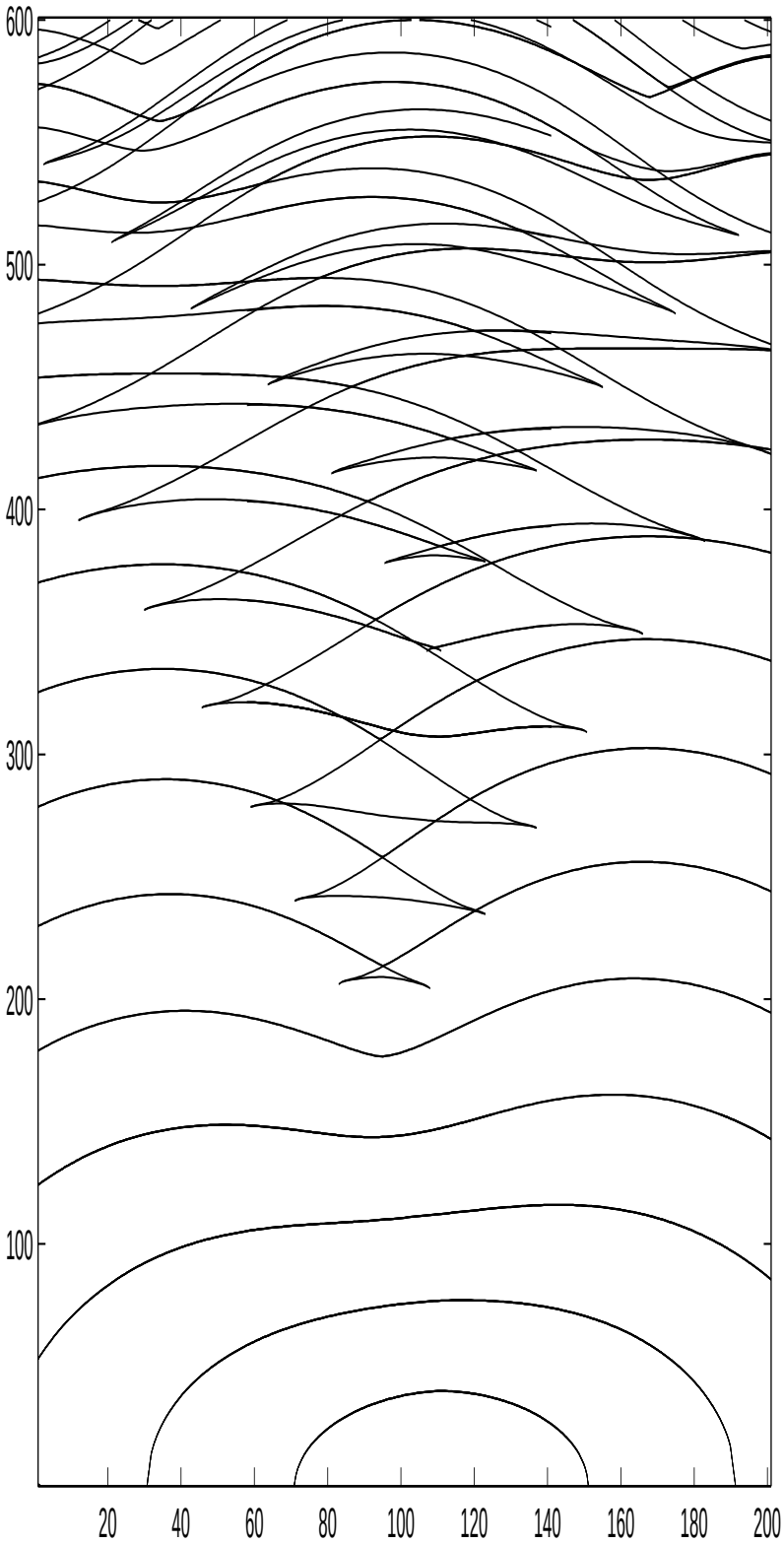

Figure 12: Geometric multi valued solution. Contour lines of ϕ

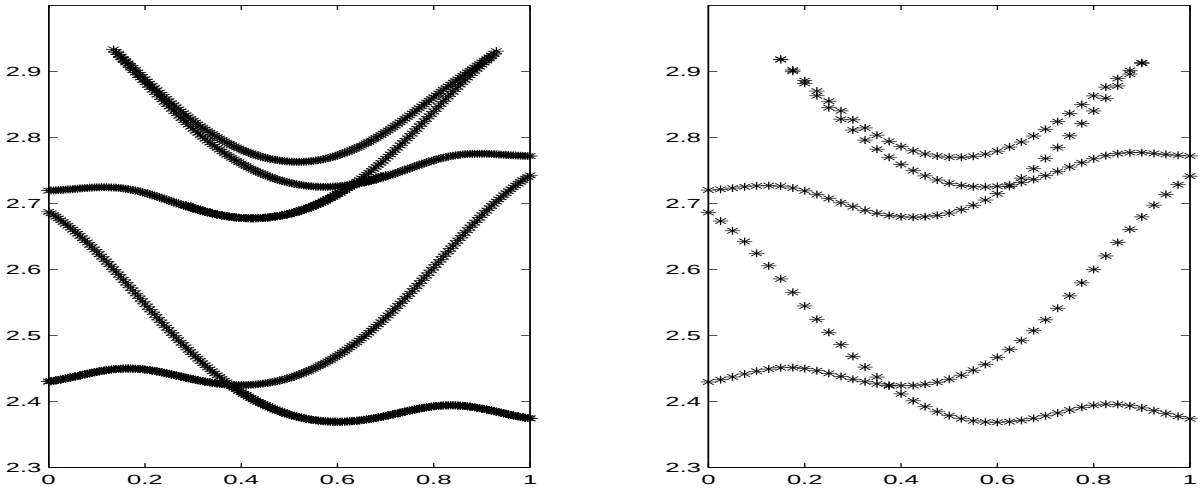

Figure 13: Comparison of the phase at $t = 1.8$. Left : our method. Right : two point ray tracing

Unit´e de recherche INRIA Lorraine, Technopôle de Nancy-Brabois, Campus scientifique,
615 rue du Jardin Botanique, BP 101, 54600 VILLERS LÈS NANCY
Unit´e de recherche INRIA Rennes, Irisa, Campus universitaire de Beaulieu, 35042 RENNES Cedex
Unit´e de recherche INRIA Rhône-Alpes, 655, avenue de l'Europe, 38330 MONTBONNOT ST MARTIN
Unit´e de recherche INRIA Rocquencourt, Domaine de Voluceau, Rocquencourt, BP 105, 78153 LE CHESNAY Cedex
Unit´e de recherche INRIA Sophia-Antipolis, 2004 route des Lucioles, BP 93, 06902 SOPHIA-ANTIPOLIS Cedex

Éditeur
INRIA, Domaine de Voluceau, Rocquencourt, BP 105, 78153 LE CHESNAY Cedex (France)
http://www.inria.fr
ISSN 0249-6399